2015

Coordinated Optimal Power Planning of Wind Turbines in a Wind Farm

Puneet Vishwakarma
University of Central Florida

COORDINATED OPTIMAL POWER PLANNING OF WIND TURBINES IN AN OFFSHORE WIND FARM

by

PUNEET VISHWAKARMA
B.S. University of Mumbai, 2005
M.S. University of Oklahoma, 2008

A dissertation submitted in partial fulfillment of the requirements
for the degree of Doctor of Philosophy
in the Department of Mechanical & Aerospace Engineering
in the College of Engineering & Computer Science
at the University of Central Florida
Orlando, Florida

Summer Term
2015

Major Professor: Yunjun Xu

ABSTRACT

Wind energy is on an upswing due to climate concerns and increasing energy demands on conventional sources. Wind energy is attractive and has the potential to dramatically reduce the dependency on non-renewable energy resources. With the increase in wind farms there is a need to improve the efficiency in power allocation and power generation among wind turbines. Wake interferences among wind turbines can lower the overall efficiency considerably, while offshore conditions pose increased loading on wind turbines. In wind farms, wind turbines' wake affects each other depending on their positions and operation modes. Therefore it becomes essential to optimize the wind farm power production as a whole than to just focus on individual wind turbines. The work presented here develops a hierarchical power optimization algorithm for wind farms. The algorithm includes a cooperative level (or higher level) and an individual level (or lower level) for power coordination and planning in a wind farm. The higher level scheme formulates and solves a quadratic constrained programming problem to allocate power to wind turbines in the farm while considering the aerodynamic effect of the wake interaction among the turbines and the power generation capabilities of the wind turbines. In the lower level, optimization algorithm is based on a leader-follower structure driven by the local pursuit strategy. The local pursuit strategy connects the cooperative level power allocation and the individual level power generation in a leader-follower arrangement. The leader, could be a virtual entity and dictates the overall objective, while the followers are real wind turbines considering realistic constraints, such as tower deflection limits. A nonlinear wind turbine dynamics model is adopted for the low level study with loading and other constraints considered in the optimization. The stability of the algorithm in the low level is analyzed for the wind

turbine angular velocity. Simulations are used to show the advantages of the method such as the ability to handle non-square input matrix, non-homogenous dynamics, and scalability in computational cost with rise in the number of wind turbines in the wind farm.

I would like to dedicate the work in this dissertation to Lord Shri Krishna. Hare Krishna.

ACKNOWLEDGMENTS

I would like to thank The National Renewable Energy Laboratory (NREL) for making their work on wind turbines accessible to researchers. I would like to thank my advisor and mentor, Dr. Yunjun Xu for being my guide and friend, I have learned a lot from him over the years and I am forever grateful to his role in my life. I would like to thank the members of my dissertation committee, Dr. Aman Behal, Dr. Jayanta Kapat and Dr. Jefferey Kauffman for accepting to be in my committee and having faith in me. I would like to thank Dr. Kuo-Chi 'Kurt' Lin for his insights and assistance in understanding wind turbine aerodynamics.

I would like to thank Dr. Ni Li and Dr. He Shen for their help and support during my PhD years. Also thanks to all my other lab mates who have helped me in big and small ways during my PhD. I am also grateful to the faculty and staff members at the Mechanical and Aerospace Department at UCF for their helpfulness and kindness.

I would like to thank my Mom, Dad, Brother and Sister for their unconditional love and support, and for giving me the freedom to pursue my own chosen path. I would like to thank Scott Delorenzo for being my American guru friend and helping me discover the knowledge not taught in schools. I would also like to take this opportunity to extend thanks to all other friends and people (*satgurus* and *upagurus*) I've met over the years for their role in my life, I have learned something from each one of them, I am a part of all that I've met.

TABLE OF CONTENTS

LIST OF FIGURES

LIST OF TABLES

LIST OF ABBREVIATIONS

LP	Local Pursuit
SCP	Speed Control Parameter
TSR	Tip Speed Ratio
VL	Virtual Leader
WT	Wind Turbine
WF	Wind Farm

CHAPTER ONE: INTRODUCTION

Motivation of Wind Farm Research

Wind energy is considered to be a cost effective and environment friendly solution to energy shortages, and with a rapid growth at the rate of around 27% per year between 2005-2009 (Pao, and Johnson 2011), it looks very promising. Wind energy, as a leading renewable energy resource, has the potential to dramatically reduce the dependency on non-renewable power generation systems by becoming a reliable companion to the same (Offshore Wind Energy 2013). The US government has plans to produce 20% of nation's energy from wind by 2030 (Schreck, Lundquist, and Shaw 2008).

Although promising in its potential, wind farms arranged in arrays suffer in power output due to aerodynamic interaction between the wind turbines. This requires wind farm control schemes that can improve the power production output and handle the aerodynamic interactions better. (Johnson, and Thomas 2009). It is shown that around 10% to 40% of wind energy output and profit is lost as a result of the interaction among wind turbines, in particularly due to wake interactions (Park, Kwon, and Law 2013, Sandia Labs News Releases 2013).

Literature Review of Cooperative Control in Wind Farms

Wind energy control research is normally focused on either individual wind turbine control or wind farm cooperative control. In individual wind turbine controls, work has been done on using linear/nonlinear feedback control techniques to track the power to be produced. An example of this can be seen in (Wang, Cai, and Jia 2013) where the researchers proposed an adaptive control strategy based on neural network to regulate blade pitch angle and rotor speed of wind turbine.

Another popular direction is the study of wind availability and the stability analysis of the system while switching between different operation regimes (Semrau, Rimkus, and Das 2015).

The approach of maximizing the power of an individual turbine renders suboptimal in terms of wind farm power production due to coupled aerodynamic effects and mechanical loadings (Spudic, Baotic, and Peric 2011, Johnson, and Thomas 2009). This beckons a scheme of coordination of individual wind turbine actions to increase the overall efficiency of the plant and reduce fatigue and loads on wind turbines (Knudsen, Bak, and Svenstrup 2014). With an increased responsibility in power generation, wind farms have other tasks to perform such as regulation and stabilization of power plants and may not be required to run at a full capacity at all times (Spudic, Baotic, and Peric 2011). Many researchers have tackled cooperative wind farm control problems. The two broad categories of approaches include (i) maximizing the power output of the wind farm, and (ii) power optimization schemes to distribute the power demand among wind turbines in a farm in terms of load reduction, e.g. in (Knudsen, Bak, and Svenstrup 2014).

Spudic et al (Spudic, Jelavic, Baotic, & Peric, 2010) described a hierarchical concept for wind farm power optimization, where wind turbines in the farm were regarded as individual power actuators with different constraints. The constraints are mainly related to the operation of wind turbine, there are speed and torque constraints on the generator and the local control system of the wind turbine has to consider these constraints. The power demand was taken as a known quantity and the supervisory control then allocates the demanded power between the wind turbines in the wind farm so as to reduce the dynamic loading on the turbines and at the same time meet the power requirement of the farm. The two levels of control were the higher level and the lower level. The higher level determines the optimal allotment of power and loads working on a slower time scale.

Whereas the lower level control makes sure the wind turbines track optimal power and loads under disturbances working on a faster time scale. An offline solution is provided by the authors for low level optimization by the use of multi parametric programming.. The model used for this work was a linear model.

Filip C.van Dam et al (van Dam, Gebraad, and van Wingerden, 2012) presented a method for controlling wind farms in a distributed framework where the wind turbines exchange information with other neighboring wind turbines taking into account the effect wake interferences. This method proved to also be feasible for real-time implementation and was shown to be effective in its test on a 60 turbine offshore wind farm. A gradient based optimization is used for power maximization. The method does not use an aerodynamic interaction model between wind turbines, instead it uses gradients approximated based on the power response, past control actions and the power response of the neighboring. For doing this a model is not required and the method is claimed to be model free.

In (Park, Kwon, and Law, 2013) the authors aim to improve the wind farm efficiency and its cost effectiveness. They do so by utilizing a cooperative game idea for the development of wind turbine power in a way that improves wind farm efficiency. The wake model used for this work is linear and the authors make use of a steepest decent algorithm to find induction factors and yaw offset angles to get an optimal mix and thereby reach the efficiency goals defined.

Researchers in (Madjidian, Kristalny, and Rantzer, 2013) employed a dynamic power coordination method, which allows wind turbines in a dispatchable wind farm to vary their power production as long as the sum of their powers meets the power demand. The turbines do this in response to local wind speed fluctuations and other turbines in a different zone compensate for this

change. The problem was divided into two parts: 1) setting optimal points for the wind turbines offline using a receding horizon strategy and 2) online coordinating of wind turbines to meet their individual power demand. The authors have also listed advantages of allowing wind turbines to adjust their own power.

Marden, Ruben, and Pao (Marden, Ruben, and Pao, 2013) took a decentralized, model free approach to achieve cooperative control of wind farms through the use of game theory. This method is claimed to be completely decentralized and can work with virtually any distributed system without the need to model the aerodynamic interaction between turbines. The control algorithm in this work aims to achieve this by letting each turbine in the farm adjust it's so called induction factor based on local information presented to it. This factor is a measure of the decrease in axial velocity to a wind turbine and is linked to the power extracted. The method proved to maximize energy production without the need for a model to describe wind turbine aerodynamic interactions. In the work the authors presented two model-free distributed learning algorithms using game theory literature and observed a 25% increase in efficiency when compared to greedy algorithms. Constraints were placed on the induction factors of wind turbines based on their position in the wind farm. Although this method gave good performances the authors admit that a highly accurate wind turbine interaction model will improve the performance further.

In (Senjyu, Ryosei, Naomitsu, Funabashi, and Sekine, 2006) the authors used pitch angle control with fuzzy neural network (FNN) to achieve power output leveling of wind farms and thus countering the problem of variations in the power productivity of wind farms. In the method the local controller solves for pitch angle using based on power output discrepancy, the cooperative level wind farm controller finds the overall error and communicates it to wind turbines in the farm,

the authors have also stated FNN methods' advantages like easy handling of nonlinear laws compared to other methods. It is shown in (Johnson and Naveen, 2009) that aerodynamic interaction between wind turbines reduces energy capture. They also showed that coordinating the operational points of aerodynamically interacting wind turbines can lead to improved energy capture. The authors have proposed a hybridized ILC/IFT (Iterative Learning Control/Iterative Feedback Tuning) controller that could reduce array losses in a wind farm. Fernandez et al (Fernandez, Battaiotto, and Mantz, 2008) proposed a strategy based on the Lyapunov theory to increase the damping of the oscillation modes of the power system in a wind farm.

In addition to the above, there have been numerous researches on the electrical side of power generation and merging of wind farms into existing grids of power generation as seen for example in (Skolthanarat, 2009) and (Sorensen, Ejnar, Hansen, Janosi, Bech, and Bak-Jensen, 2002).

Although there have been many work in recent years focusing on the cooperative control of wind turbines, as reviewed above, there is still plenty of room for improvement in this area. For example, most of the recent work focuses on the use of linearized wind turbine models (Munteanu, Cutululis, Bratchu, and Ceanga 2005) for optimization purposes; this can lead to errors as some wind turbine operating modes in linearized models do not match well with real nonlinear phenomena. Furthermore, the work in coordinated wind farm control often ignores structural deflection constraints of individual wind turbines (Spudic, Jelavic, Baotic, and Peric 2010). In some wind farm cooperative control work as seen in (Soleimanzadeh, Brand, and Wisniewski 2011), the algorithm has a high computational cost when applied to larger wind farms and is not scalable with increase in the number of wind turbines.

Therefore, a wind farm cooperative control method is needed which can work with a more

accurate nonlinear wind turbine model. There also a need for the method to take into consideration the effects of wake interaction between the wind turbines and regard that as coupled constraints in the power planning of the wind farm. As structural loading on wind turbines over a period of time can cause fatigue and wear and tear it is important that loadings on the turbine and stress experienced by turbine components are kept under check by placing constraints on them when optimally planning the power output distribution in a wind farm. Method also needs to be scalable in terms of CPU time, with an increase in demand and size of wind farms a scalable algorithm for power distribution is required. The optimal cooperative power planning in this work is divided into a hierarchical structure which consists of two levels, cooperative and individual. The cooperative level algorithm handles the objective of optimally allocating power to the wind turbines while considering the coupled constraint of wake interaction between wind turbines, as well as uncoupled constraints of power production limits of individual wind turbines based on wind turbine properties and available wind speeds.

The individual level algorithm is to minimize the differences between the actual power generated and the allocated power demand while considering individual wind turbine constraints such as thrust and torque on the rotor, the rotor speed, and the tower deflection.

A leader follower structure is used in connecting the cooperative and individual level algorithms. The recently studied cooperative control strategy (Xu, Remeikas, and Pham 2013) inspired by the local pursuit strategy found in ants (Hristu-Varsakelis and Shao 2004) will be further enhanced to govern the relationship between the power generation in virtual leader power and individual wind turbine.

Dissertation Outline

The following sections summarize each chapter of this dissertation and their contributions.

Chapter 2: In this chapter, individual wind turbine model, wake interaction model and tower deflection model are presented. The wind turbine model is simulated and the results are validated with the results of NREL. A section is dedicated to different options of influencing power output of a wind turbine.

Chapter 3: In this chapter, the cooperative control framework for the wind farm is described. The performance indices of the upper (cooperative) and lower (individual) level optimization problem are presented. The overall structure of the optimization algorithm is also presented in this chapter.

Chapter 4: In this chapter lower level wind turbine planning is discussed. The wind turbine power output regulation using the modified local pursuit strategy is presented in this chapter, along with the rotor speed stability proofs and the lemmas connected with it. These are followed by the algorithm for the propagation of model and the individual wind turbine power generation algorithm.

Chapter 5: In this chapter, higher level power generation planning is outlined. The derivation of equivalent higher level performance index for use in quadratic programming solver is presented. The algorithm for calculation of wind turbines' power ranges is also presented followed by the algorithm for the quadratic programming optimization. Finally the overall optimization algorithm is outlined in this chapter.

Chapter 6: In this chapter, the cooperative control strategy is simulated and the results are presented. The chapter describes the simulation settings used for the overall optimization. The

simulations presented in the chapter can be divided into two categories 1) individual wind turbine optimization and 2) coordinated wind turbine optimization. In the individual case three different scenarios are simulated a) varying wind speeds b) varying allocated power and c) varying initial power of wind turbines. In the coordinated optimization simulations are carried out for three different sizes of wind farm arrays, a) 2x2 b) 4x4 and c) 5x5. Finally the results are summarized and presented.

Chapter 7: In this chapter different directions for the future of this work are discussed and conclusions are drawn about the virtual leader method used.

Contributions

The main contributions of this work are as follows.

1) In the cooperative power planning of the wind farms both coupled and uncoupled constraints are considered. Wake interaction among wind turbines in a wind farm is responsible for coupled constraints. This interaction is dependent on the wind speeds available, the operation mode of the wind turbine in terms of pitch angle setting and rotor speed which will influence the thrust on the wind turbine, and also the distances between the wind turbines which can be a function of the layout of the wind farm. In the uncoupled constraints individual wind turbine constraints are considered. These include the rotor torque and rotor speed constraints. Also included here are the limits placed on the thrust force and tower deflection.
2) In this work a nonlinear wind turbine model is used, which is closer to the real system and free from errors outside of linearization regions.
3) The method presented in this work is capable of handling non homogeneous models and is

independent of the particular models used in the simulations performed. The wake model can also be replaced to suit the layout of the wind farm much better. For the offshore wind farm arrays, the Jensen wake model was sufficient but for the more complicated land based wind farms which involve terrains, a more suitable model can be used in the method.

4) The power output of wind turbine when driven by the modified local pursuit strategy is guaranteed to be asymptotically stable. The rotor speed steady state value when the power is driven by the modified local pursuit strategy is also asymptotically stable. Typically asymptotic stability is not studied in such open loop optimal planning problems.
5) In the coordinated power planning the work also considers tower deflection which is a measure of the stress experienced by the wind turbine structure. Tower deflections are not usually considers in real-time coordinated power planning of wind turbines in wind farms.
6) The upper level of the cooperative power planning algorithm is capable of rapid planning in the allocation of power to the wind turbines in terms of CPU time. This is evident from the simulation results of this work.
7) The algorithm presented in this work is scalable in terms of CPU time as the number of wind turbines in a wind farm increases. The method is decentralized and each wind turbine only refers to the virtual leader wind turbine. This is evident from the simulation results as the CPU time of optimization algorithm increases only slightly as the number of wind turbines is increased.
8) The method is customized to handle non-square input matrices while finding the inverse dynamics as compared with the method used in (Xu, Remeikas, and Pham 2013). The approach is based on special constraints shown in a typical wind turbine model.

CHAPTER TWO: WIND TURBINE MODEL AND SIMULATION

Individual Wind Turbine Model

The nonlinear wind turbine model adopted from (Wang, Cai, and Jia 2013) consists of the blade pitch actuator dynamics and the wind turbine rotor dynamics

$$\begin{aligned}\dot{\boldsymbol{x}} &= f(\boldsymbol{x}) + g(\boldsymbol{x})u \\ &= \begin{bmatrix} \dfrac{\rho\pi R^2 C_p(\lambda,\beta)V^3}{2J\omega_r} - \dfrac{an_{gb}^2\omega_r}{J} - \dfrac{bn_{gb}}{J} \\ \dfrac{-\beta}{T_\beta} \end{bmatrix} + \begin{bmatrix} 0 \\ \dfrac{1}{T_\beta} \end{bmatrix}\beta_r \end{aligned} \tag{1}$$

Here the state variables $\boldsymbol{x} = [\omega_r, \beta]^T$ are the rotor angular velocity and the blade pitch angle, and the control variable β_r is the blade pitch angle reference input. $C_P(\lambda,\beta)$ is the rotor power coefficient. $\lambda = \omega_r R/V$ is the tip speed ratio. ρ, R, V, $J = J_{rotor} + n_{gb}^2 J_{generator}$, n_{gb}, and T_β are the air density, the rotor radius, the average wind speed, tip speed ratio, the gear box ratio, the equivalent shaft inertia, and the time constant of the pitch servo system, respectively. The data and coefficients used in this model are selected from a 5 MW capacity offshore wind turbine (Jonkman, Butterfield). The constants a and b are the parameters in the linearized generator torque model $T_g = a\omega_g + b$ (Wang, Cai, and Jia 2013), where the generator speed is given as $\omega_g = n_{gb}\omega_r$. It is worth noting that the input matrix in Eq. (1) is non square. It has 2 state variables but 1 control variable. The outputs of the model $\boldsymbol{h}(\boldsymbol{x})$ include the power extracted from the wind P, the torque experienced by the low speed shaft T, and the thrust experienced by the rotor F as

$$\boldsymbol{y} = \boldsymbol{h}(\boldsymbol{x}) = \begin{bmatrix} P \\ T \\ F \end{bmatrix} = \begin{bmatrix} 0.5\rho\pi R^2 V^3 C_P(\lambda,\beta) \\ 0.5\rho\pi R^2 V^3 C_Q(\lambda,\beta) \\ 0.5\rho\pi R^2 V^2 C_T(\lambda,\beta) \end{bmatrix} \tag{2}$$

in which $C_P(\lambda,\beta)$, $C_Q(\lambda,\beta) = C_P(\lambda,\beta)/\lambda$, and $C_T(\lambda,\beta)$ are the rotor power coefficient, the rotor torque coefficient, and the rotor thrust coefficient, respectively. The coefficients of the 5 MW offshore NREL wind turbine as described in (Jonkman, Butterfield, Musial, and Scott 2009) are used in this work. The cut-in and rated wind speed for such a wind turbine are 8 m/s and 11.4 m/s respectively. For the wind turbine model simulation, start up and shut down scenarios were not included.

The limitations on rotor speed, pitch angle, rotor torque, and thrust force are

$$\omega_{r,\min} \le \omega_r \le \omega_{r,\max}, 0 \le \boldsymbol{T} \le \boldsymbol{T}_{\max}, 0 \le \boldsymbol{F} \le \boldsymbol{F}_{\max} \tag{3}$$

To make extraction of pitch angle easy from a known C_p and λ, a mathematical equation is used (Hui & Bakhshai, 2008), this equation is given as,

$$C_p(\lambda,\beta) = c_1\left(c_2/\lambda_k - c_3\beta - c_4\right)e^{\frac{-c_5}{\lambda_k}} + c_6\lambda_k \tag{4}$$

$$\frac{1}{\lambda_k} = \frac{1}{(\lambda + 0.08\beta)} - \frac{0.035}{\beta^3 + 1} \tag{5}$$

where, $c_1 = 0.5176$, $c_2 = 116$, $c_3 = 0.4$, $c_4 = 5$, $c_5 = 21$, and $c_6 = 0.0068$. The C_p value calculated using Eqs. (4) and (5) matches well with the values obtained from the FAST and AeroDyn packages of NREL (Jonkman, Butterfield, Musial, and Scott 2009)

The Jensen wake model (Renkema 2007) is used to calculate the velocity deficit downstream between wind turbines in the farm, which permits fast calculations and is commonly used in

commercial wake calculation programs.

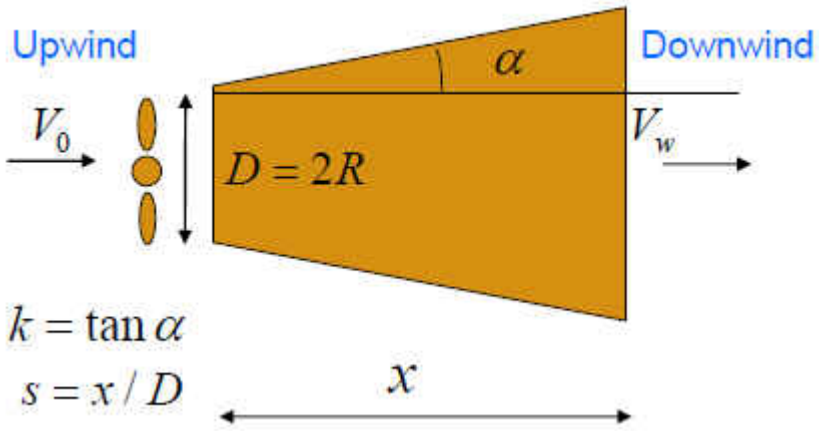

Figure 1 Jensen wake model

The equation for calculating the wind speed in the wake at a distance x is given as follows (Renkema 2007) .

$$V_w(x) = V_0 \left\{ 1 - \frac{\left(1 - \sqrt{1 - C_T}\right)}{\left(1 + k\left(\frac{x}{R}\right)\right)^2} \right\} \tag{6}$$

Here V_0 and k are the incoming wind speed and the entrainment constant, and R is the rotor radius.

The thrust force acting on the wind turbine rotor plane causes the oscillation of the tower.

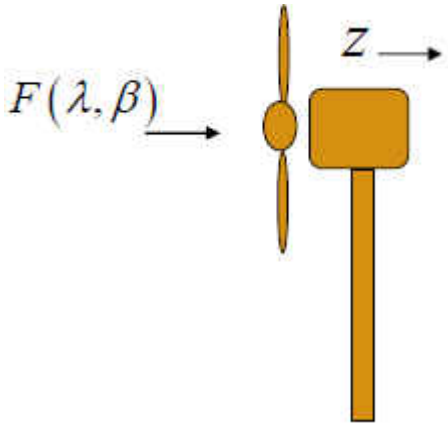

Figure 2 Wind turbine tower deflection

The second order system in Eq.(7) describes the tower deflection (nodding) in the fore-aft direction (Spudic, V., Jelavic, M., Baotic, M. and Vasak, M., 2010),

$$m\ddot{z} + d\dot{z} + cz = F(\lambda, \beta) \tag{7}$$

in which z is the displacement of tower top in the direction of the wind, F is the thrust force acting in the rotor plane and assumed to be concentrated in the center of the rotor hub. The other parameters in the equation are the modal mass denoted by m, the modal damping denoted by d, and the modal stiffness of the tower denoted by c. The displacement of tower top should be $|z| \le z_{\max}$. Tower nodding can be modeled adequately by using the two modes or two modal frequencies. The model in this work is used for planning and control purpose only and hence only the first mode of vibration is considered. The second mode is about 6 times greater than the first modal frequency and can be safely neglected in our work. (Jelavic, Peric, and Petrovic, 2007). The modal elements of Eq. (7) are based on the first modal frequency of tower vibration in fore-aft direction and can be found with the following equations (Jelavic, Peric, and Petrovic, 2007),

$$d = 2\zeta_t \omega_{0t} m \tag{7a}$$

In the Eq. (7a) above, ζ_t is the structural damping of the wind turbine tower. Steel is used for building the tower in case of commercial MW capacity wind turbine towers and this value for steel is generally taken to be 0.005. In Eq. (7a), m is the modal mass of the wind turbine tower. The modal stiffness of the wind turbine tower is calculated using the following equation (Jelavic, Peric, and Petrovic, 2007),

$$c = \omega_{0t}^2 m \tag{7b}$$

Again in Eq. (7b) above, ω_{0t} is the first modal frequency of the tower vibration. The modal mass (m) of the wind turbine tower was calculated by adding the nacelle mass of the wind turbine (including the rotor) and the top equivalent mass of the tower. (Van der Hooft, Schaak, and Van Engelen, 2003). The data for these calculations were taken from (Jonkman, Butterfield, Musial and Scott, 2009).

The coefficient of power (C_P) is a nonlinear function and is wind turbine specific. It is a dimensionless ratio of the extracted power to the kinetic power available in the undisturbed wind stream. The maximum theoretically possible value for the coefficient of power is 0.596 and is known as the Betz limit. In real wind turbines this number is usually around 0.45 and this drop is due to inefficiencies and losses in different turbine configurations, number of blades, the blade profiles and different designs. Coefficient of power is dependent on tip speed ratio (λ) and pitch angle (β). The power coefficient curve for the chosen wind turbine (NREL 5 MW) is shown below in relation to pitch angle and tip speed ratio.

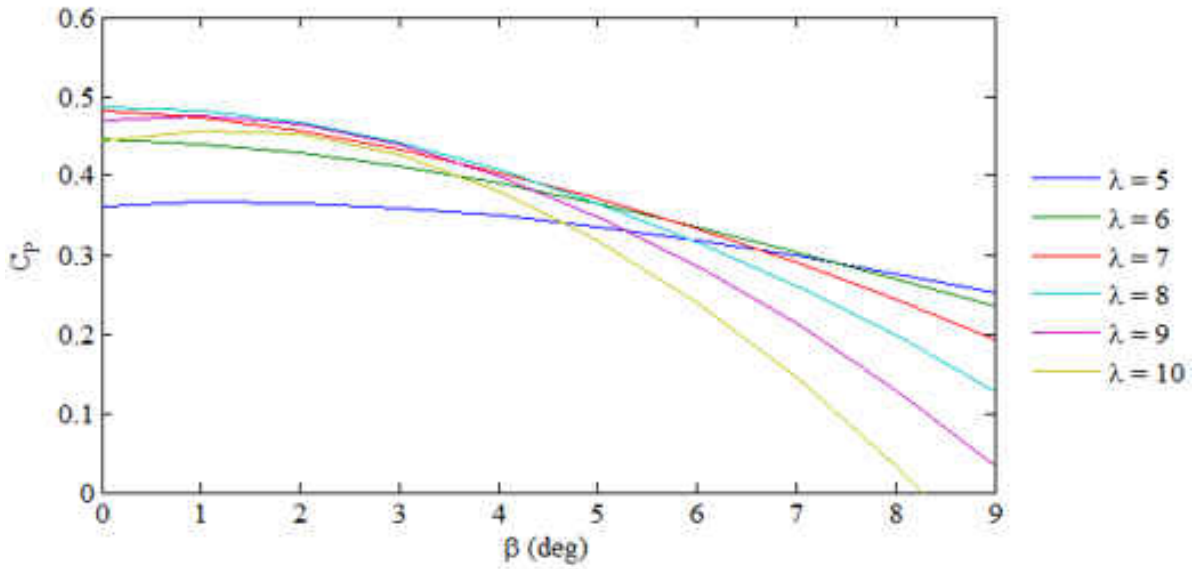

Figure 3 Coefficient of power v/s pitch angle

Fig. (3) shows the variation of pitch angle for a range of values for tip speed ratio in normal operation of wind turbine. The constant lines in the figure represent the tip speed ratio values. The maximum coefficient of power value for a given tip speed ratio is attained at 0 degree pitch angle. For the NREL wind turbine chosen in this work this value is near 0.48. We can change coefficient of power by adjusting pitch angle as evident from the figure.

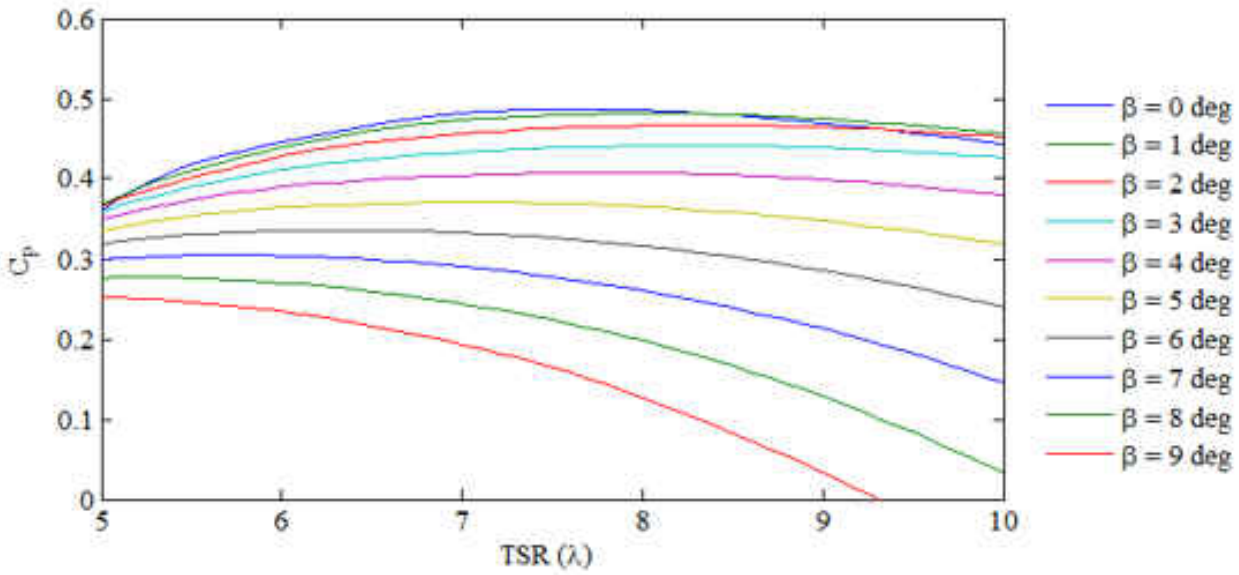

Figure 4 Coefficient of power v/s tip speed ratio

Fig. (4) shows the variation of coefficient of power with the tip speed ratio within a normal operating range. The constant lines in Fig. (4) represent the pitch angles. A given wind turbine will operate at its maximum coefficient of power at a certain mix of tip speed ratio and blade pitch angle. The wind turbine in consideration achieves the maximum coefficient of power at 0 deg pitch angle and a tip speed ratio value of 7.55. Pitch angle is independent, whereas the tip speed ratio depends on wind speed and the rotor speed, to maintain the tip speed ratio at the optimal setting the rotor speed is varied in relation to the incoming wind speed. It is possible to adjust the power of the wind turbine by adjusting just the tip speed ratio, and the change in coefficient of power with respect to tip speed ratio can be seen in Fig. (4).

Similar to coefficient of power, the coefficient of thrust is also a nonlinear wind turbine specific function and is used to find the thrust force experienced by the wind turbine rotor. The coefficient of thrust curves are shown in the figure below.

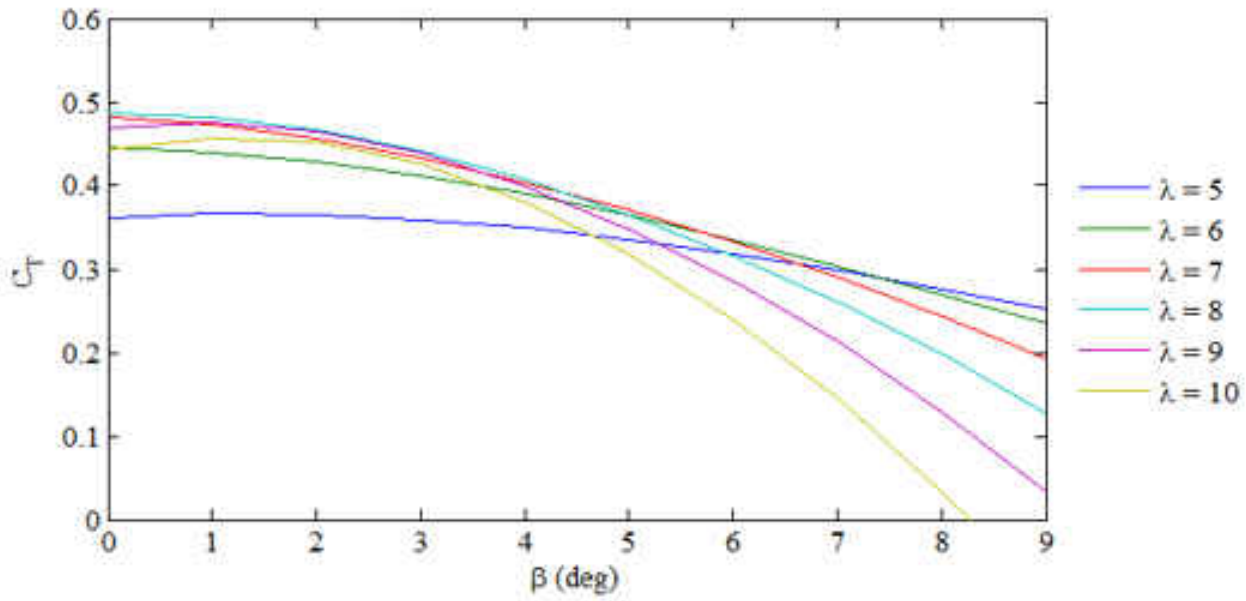

Figure 5 Coefficient of thrust v/s pitch angle

Fig. (5) shows the variation coefficient of thrust in relation to the blade pitch angle within a normal operation range. The individual lines represent the tip speed ratio values. For pitch angles closer to the maximum power setting the wind turbine rotor experiences more thrust as there is more surface area contact between the blades and the incoming wind. Thrust on the rotor increases the structural loads of the tower and the wind turbine blades. Hence it is important to be able to influence it by varying the pitch angle. The trends in variation of thrust with respect to blade pitch can be seen in the Fig. (5) above.

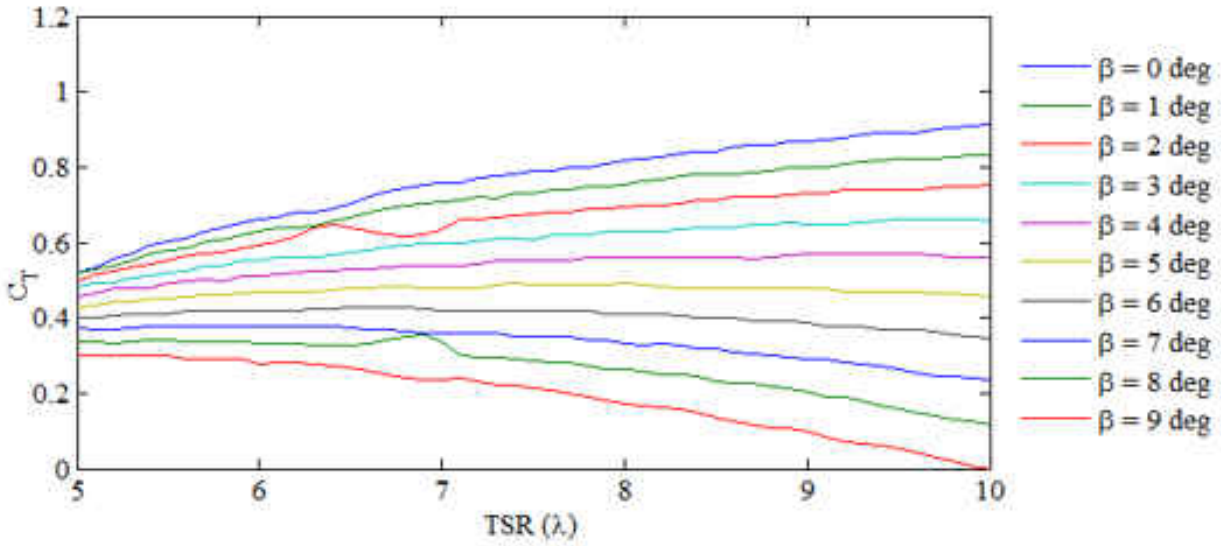

Figure 6 Coefficient of thrust v/s tip speed ratio

Similar to Fig. (4), Fig. (6) shows the variation of coefficient of thrust with respect to the tip speed ratio.

The nonlinear wind turbine function values were obtained from NREL's (Jonkman, Butterfield, Musial, and Scott 2009) data, and were used for simulation of the wind turbine model in this work.

Power Control Options

For an available wind speed the wind turbine mechanical power output can be manipulated by the following methods,

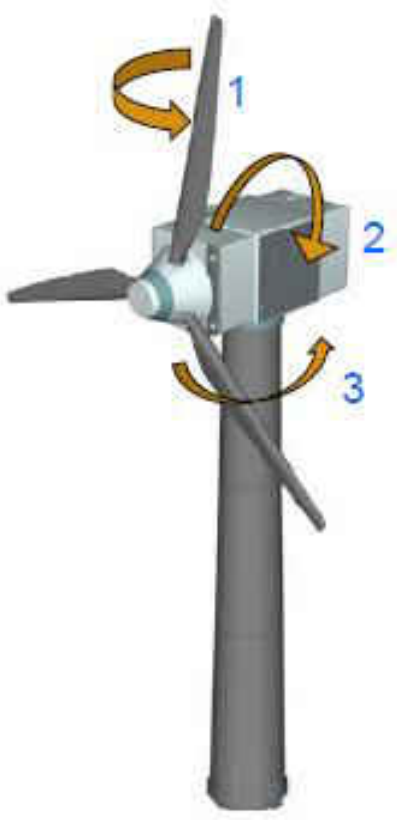

Figure 7 Power control options (Wind turbine 3D model, 2015)

1) Collective blade pitch angle: By adjusting the pitch of the blade the coefficient of power of the wind turbine (C_P) can be influenced, which in turn influences the power. The maximum power output setting for the NREL 5 MW capacity wind turbine is 0 deg. Positive increment in the angle of blade pitch is known as feathering (Hau, 2012) and is a common method to limit power output in wind turbines. The model adopted in this work has provision to adjust the blade pitch angle. The control variable in the model (Eq. (1)) is

the reference pitch angle (β_r) which determines the pitch angle of the wind turbine blades. Changing the pitch angle for a given tip speed ratio changes the coefficient of power value, the variation of the C_P value with pitch angle for the wind turbine used in this work can be seen in Fig.(3).

2) Generator torque control: The power output can also be changed by adjusting the electrical torque of the generator. By changing the electrical torque by using power electronics the mechanical torque of the wind turbine rotor is changed, which affects the rotor speed. Change in rotor speed brings about a change in the tip speed ratio of the wind turbine rotor (λ). As the coefficient of power is dependent on tip speed ratio, the power can be adjusted by changing the generator toque. This is a common method of power control used in variable speed wind turbines and the model adopted in the current work has provision to achieve this. The variation in tip speed ratio changes the C_P value of power in Eq. (2), the variation of C_P for a given pitch angle can be seen in Fig. (4).
3) Nacelle Yaw: The wind turbines power can also be influenced by yawing the nacelle of the wind turbine, this adjustment moves the rotor out of the wind direction, which affects the power output. The yawing of wind turbine rotor out of wind during low or high wind speed condition is known as furling. Most aerodynamic simulations of wind turbine neglect nacelle yaw due to the really low rate (1 deg/sec). The model in this work assumes the rotor plane is yawed into the direction such that wind velocity is normal to the plane of rotation.
4) Other factors which affect the power output are the air density and size of the rotor. As can be seen from Eq. (2) the power output of a wind turbine is proportional to the air density

and squarely proportional to the rotor radius. Another important factor is tower height, although not directly present in the power equation, a taller tower is much better equipped to capture free stream wind this is especially true for land cases where structures around the wind turbine like trees and buildings can obstruct the wind and a taller tower is needed to overcome this problem. In offshore cases a sufficiently high tower is capable of producing the ideal power for a given wind speed, a 1:1 ratio between the tower height and rotor diameter is a common rule of thumb for such offshore wind turbines (Gipe, 2004)

Simulation Settings

The simulation is carried out on a laptop, running Intel® Core i7-2620M with a processor speed of 2.7 GHz and a 6 GB RAM. The properties of the wind turbine are adopted from (Jonkman, Butterfield, Musial, and Scott 2009) as shown in Table 1.

Table 1 Properties of 5 MW wind turbine

Parameter Definition	**Number**
Gear box ratio (n_{gb})	97
Generator inertia (J_g)	$534.12\ kg \cdot m^2$
Rotor inertia (J_r)	$115920\ \ kg \cdot m^2$
Equivalent shaft inertia ($J = J_r + n_{gb}^2 J_g$)	$5.14 \times 10^6 kg / m^2$
Air density (ρ)	$1.2041\ \ kg / m^3$
Rotor radius (R)	$63\ m$

Parameter Definition	**Number**
Pitch actuator time constant (T_β)	0.2 sec
Modal mass of wind turbine tower (m)	587460 kg
Modal damping of the wind turbine tower (d)	1903.37$N/(m/s)$
Modal stiffness of the wind turbine tower (c)	61669.20 N/m
Tower height (h)	87.6 m

Wind Turbine Model Simulation

The wind turbine model used in this work was validated with the results of NREL 5 MW wind turbine (Jonkman, Butterfield, Musial, and Scott 2009). For the validation 3 cases were tested.

Case 1

In the first case the wind turbine model is simulated to match the maximum power setting ($\beta = 0\,\text{deg}$) at the rated wind speed of 11.40 m/s. The torque parameters, a and b used for validation were taken from (Jonkman, Butterfield, Musial, and Scott 2009). The results matched with NREL results for the same setting and are displayed in the following figures.

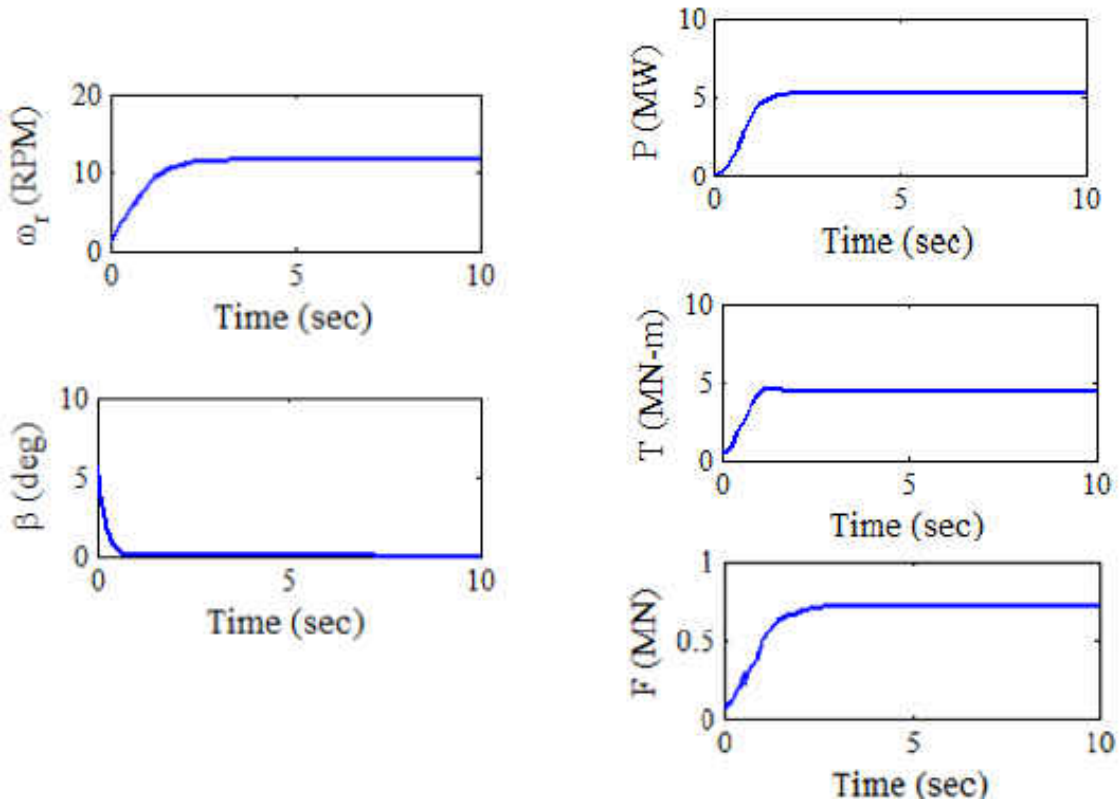

Figure 8 Model validation case 1

For the rated wind speed of 11.4 m/s, the NREL 5 MW capacity wind turbine is expected to produce 5 MW in electrical power with a generator efficiency of 94.4% the rated mechanical power at the rated capacity is around 5.2 MW, the results in this case of validation matched these numbers for the rated operation conditions. The rated power is defined at the maximum power point setting of the blade pitch angle and for this wind turbine it is 0 deg. The wind turbine blade pitch actuator time constant of 0.2 sec can be seen at work in the pitch angle plot. The rotor speed at this setting also matched well with the NREL data and is at about 12.1 RPM. The torque and thrust values at this rated setting were able to match the NREL values of around 4.2 MN-m and 0.8 MN respectively.

Case 2

In the second case the wind turbine model is simulated to experience wind speeds higher than the rated value. A wind speed of 13 m/s was chosen, to obtain the rated power in this high wind speed condition a pitch reference angle of 7 deg was applied to maintain the power output at the rated value. The results of this case are shown in Fig. (9).

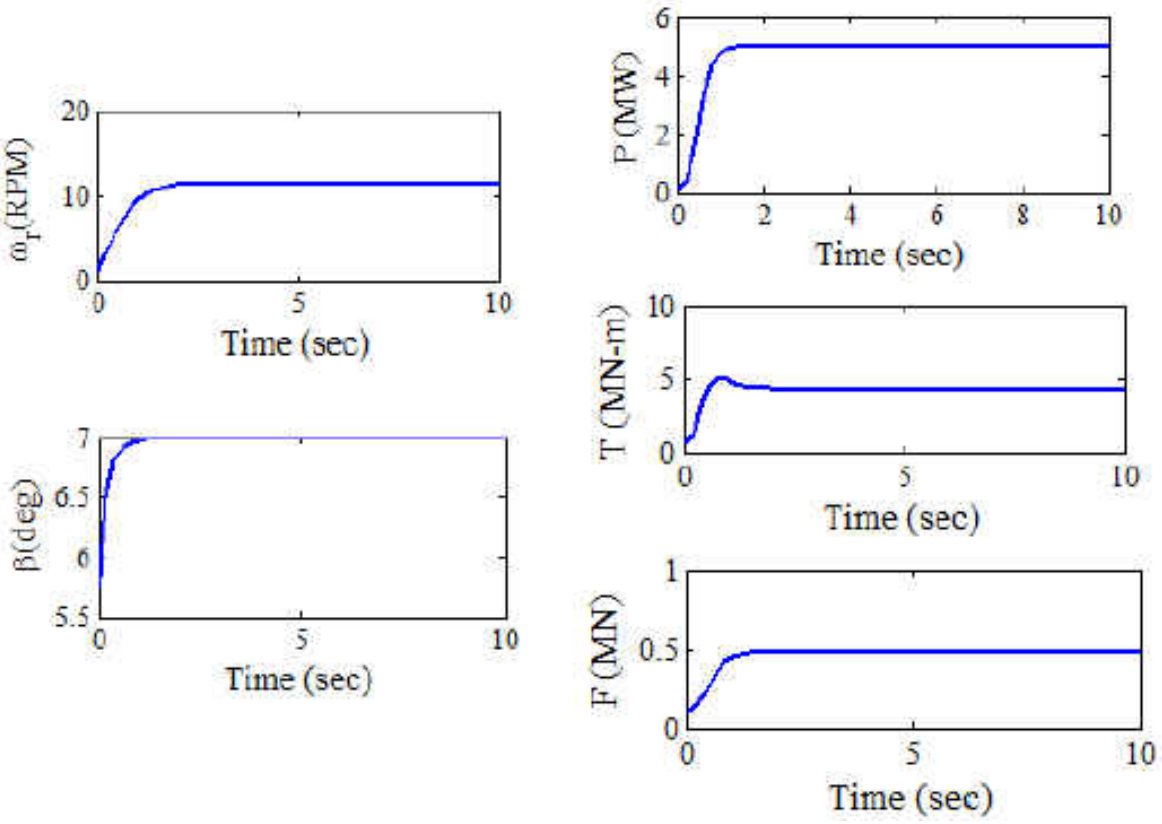

Figure 9 Model validation case 2

In wind speeds higher than the rated wind speed, it is common to use pitching also known as feathering to limit the power to the rated value. For the wind speed selected for this case based on NREL results a blade pitch angle of about 7 deg is needed to limit the power to the rated value, a pitch angle reference of 7 deg is given to the wind turbine model and the steady state

results match with the rated operation values. The mechanical power is at 5.2 MW and rotor torque at around 4.2 MN-m. When the rotor blades pitch away from the maximum setting to positive values, the wind turbine rotor experiences less thrust, and for this setting the rotor thrust of roughly 0.5 MN matches the NREL setting for 13 m/s wind speed and 7 deg pitch angle. The rotor speed achieved with this pitching maneuver is around the 12.1 RPM which matches the with the rated power results.

Case 3

In the third case the wind turbine model is simulated to experience lower wind speed than the rated value. A wind speed of 8 m/s was chosen, to obtain the maximum possible power in this low wind speed condition a pitch reference angle of 0 deg was applied. The results of this case are shown in Fig. (10).

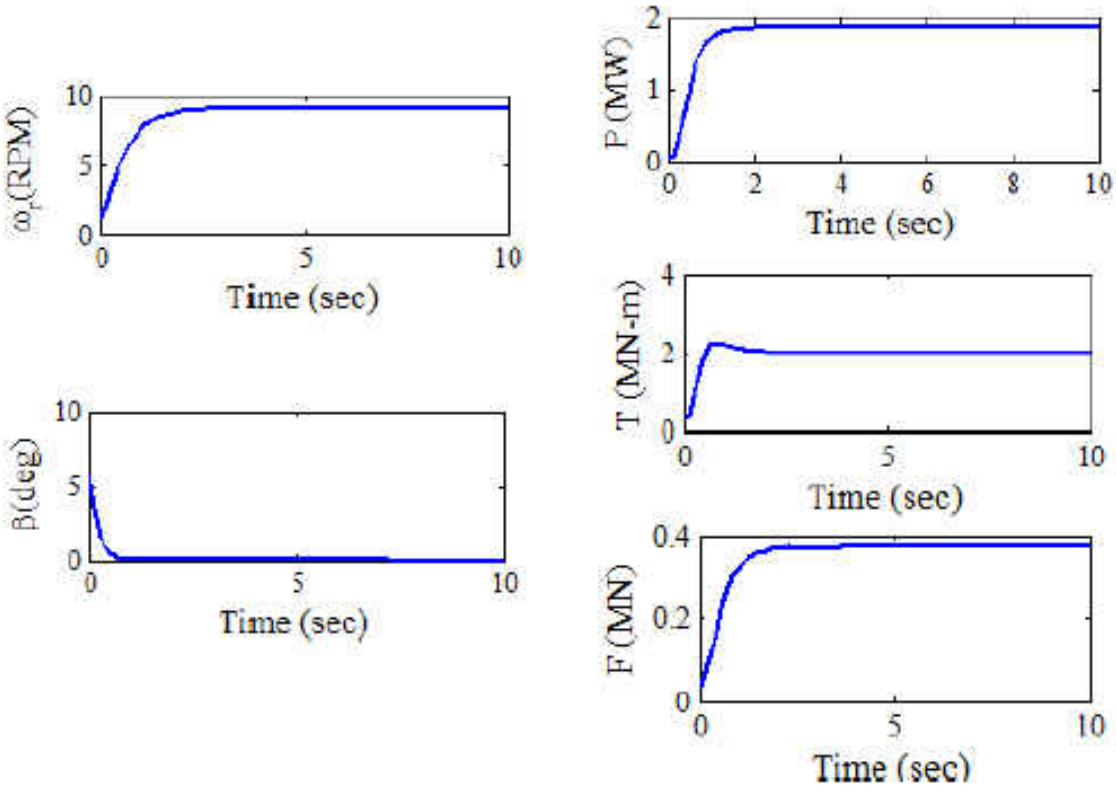

Figure 10 Model validation case 3

In low wind speeds the wind turbine experiences lower thrust from the incoming wind, the rotor thrust for this case is around 0.4 MN which is close to the NREL results for similar combination of pitch angle and wind speed. The maximum power that can be produced safely at this wind speed is around 2 MW and the rotor torque slightly less than 2 MN-m. In normal operation when the wind speeds are lower than the rated value the strategy is to maximize power, unless the power demand is also dropped.

All the three cases matched well with the results presented in (Jonkman, Butterfield, Musial, and Scott 2009)

The coordinated optimal power planning method outlined in this work is independent of the models used in the work. And other models can be used to carry out this method. The method is capable of handling non homogeneous models.

The method presented in this work is can be applied to any definition of wind turbine and is not limited to the 5 MW offshore wind turbine used for the simulation. The wind turbines in the wind farm can also be of different specification and will not affect the method used. The total maximum power that can be generated will vary depending on the capacity of the wind turbines in the wind farm but the method will remain unaffected. Similarly the wake model used can be different depending on the layout and accuracy of wake calculation needed. The method can also accommodate other constraints that may apply for a different model used, for example blade deflection constraints can be added.

CHAPTER THREE: COOPERATIVE OPTIMAL POWER CONTROL PROBLEM FORMULATION

Power Generation Optimization in Individual Wind Turbine

The performance index to be optimized in each of the wind turbines is

$$J_i = \int_0^{t_f} \left[W_1 (P_i - P_{i,d})^2 + W_2 F_i^2 + W_3 T_i^2 \right] dt, \;\; i = 1, \ldots, N_w \tag{8}$$

We assume that there are N_w wind turbines in the farm, and $W_k, k = 1,2,3$ are user defined weights for each component in the performance index. P_i and $P_{i,d}$ are the actual and allocated power of the i^{th} follower wind turbine in the prediction horizon $[0, t_f]$. F_i and T_i are the thrust force acting in the rotor plane and the rotor torque of the i^{th} wind turbine.

The equality constraints include the nonlinear, under-actuated dynamics Eq. (1), and initial condition $\omega_{r,i}(t_0)$ and $\beta_i(t_0)$; while Eq. (3) and the fore-aft tower deflection limitation are regarded as the inequality constraint.

Varying emphasis can be placed on the components of the performance index depending on what is more important to the algorithm. If the goal is to keep the loading on the wind turbine low more weight can be added to the force and/or the torque terms and the weights on power term can be reduced or neglected as the modified LP equation used for driving power is asymptotically stable and expected to reach its desired value. In case the wind turbine is not getting enough wind to produce the desired power emphasis can be placed on the power part of the performance index and the loading weights can be ignored or relaxed.

Power Allocation in Wind Farms

In the wind farm cooperative level power allocation, the wind speed available to upwind turbines and the distances between the upwind and downwind turbines is known. At a particular time, the power grid network needs a total of P_{tot} from this farm. The performance index in the cooperative level is the difference between the power demand and the overall power generated by each wind turbine.

$$\boldsymbol{J} = \left(\sum_{i=1}^{N_w} P_i - P_{tot} \right)^2 \tag{9}$$

The power allocated to wind turbine i is limited by its power generation capability $[P_{i,\min}, P_{i,\max}]$, which depends on the ranges of its incoming wind, pitch angle and tip speed ratio.

In the above equation, N_w is the number of wind turbines, $\boldsymbol{P_i}$ is the power to be allocated to i^{th} wind turbine by the wind farm level controller.

The overall architecture of the wind farm power planning algorithm can be summarized in the Fig. (11) below.

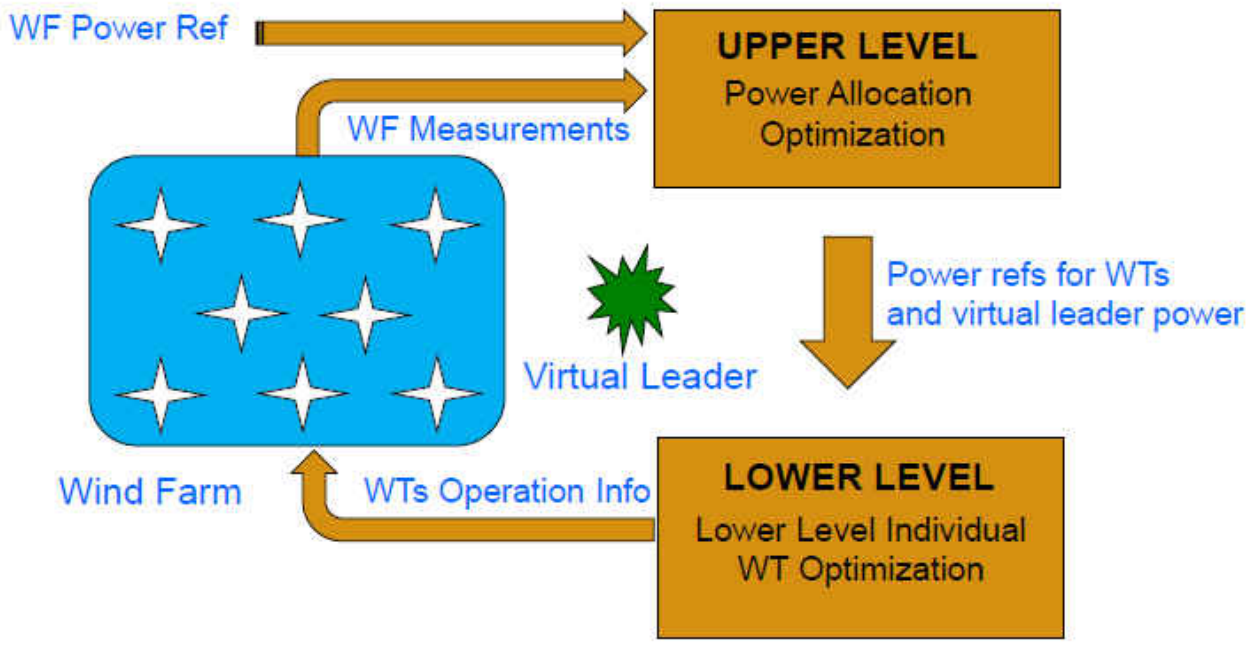

Figure 11 Overall architecture for optimization

The structure of the hierarchal wind farm optimal power planning algorithm consists of two main parts. 1) Upper (Higher) level, 2) Lower (Individual) level. The total power demand from the wind farm is known, and sent to the higher level part of the optimization algorithm. Also known to the higher level are the wind farm measurements, these include the wind speed available at the front row of wind turbines, and the layout information which include the number of wind turbines present (N_w) the distances between wind turbines and their power production capacities. The power production capacity depends on the size of the wind turbine rotor and its coefficient of power information. With these information at hand the upper level finds out the velocity deficits at subsequent rows of wind turbines using the Jensen's wake model given in (6), and calculates the range of power available to wind turbines $[P_{i,\min}, P_{i,\max}]$, with the bounds and total power known the upper level solves the cooperative level performance index in Eq. (9). In

the higher level optimization, the goal is to match the total wind farm power demand and the algorithm tries to match the demand by solving the performance index in Eq. (9). After solving the power to be allocated to each wind turbine is sent to the lower level. Also sent to the lower level is the virtual leader wind turbine power information. This is an imaginary wind turbine and part of the modified local pursuit strategy used to drive the real wind turbines' power output. Its power for optimization purpose is taken to be the average of total power demand with respect to the total number of wind turbines. The modified local pursuit strategy which will be discussed in more detail in the next chapter forms the connection point between the upper and lower level optimization algorithms. The lower level then proceeds to minimize the performance index in Eq. (8) and solves for the reference pitch angle to be sent to wind turbines for achieving the allocated power. The operation info of the wind turbines is then sent back to upper level again. The lower level algorithm will be discussed more in detail in chapter 4.

CHAPTER FOUR: LOCAL PURSUIT BASED INDIVIDUAL WIND TURBINE OPTIMAL CONTROL

Power Output Regulation

In the lower level optimization performance index as given in Eq. (8) the P_i term is the actual wind turbine power and it is proposed to be driven by the modified local pursuit strategy. The origin of local pursuit strategy lies in the phenomenon observed in foraging ants for finding optimal and/or feasible path (Hristu-Varsakelis and Shao 2004). This method follows a leader and follower structure. The leader can be a virtual one which is true in present case of the wind turbines. In the original local pursuit (LP) strategy a follower ant points its velocity in the direction of the leader ant to achieve a minimum time performance. The LP rule is given as (Hristu-Varsakelis and Shao 2004),

$$\dot{\boldsymbol{x}}_{i,p}(t) = v_i\left[\boldsymbol{x}_{VL,p}(t) - \boldsymbol{x}_{i,p}(t)\right], i = 1,..,n_v \tag{10}$$

The power output of each wind turbine is proposed to be driven by a modified local pursuit strategy (Xu, Remeikas, and Pham 2013)

$$\dot{P}_i = v_i(P_{VL} - P_i) + v_i\Delta_i + \dot{P}_{VL}, i = 1,...,N_w \tag{11}$$

in which P_{VL} is the power output of leader that can be a virtual wind turbine, and the value can be the average power generated by N_w wind turbines in the farm as $P_{VL}(t) = P_{tot} / N_w$. The constant term Δ_i in a planning horizon is the power output bias of wind turbine i from P_{VL}. There are different approaches to drive the power of each wind turbine towards its allocated value.

Following Eq. (11) is just one approach. In this approach, the actual wind turbine power will follow a first order trajectory without an overshoot. Additionally, the speed control parameter

(SCP) v_i determines how fast the power output P_i will converge to its desired value $P_{VL} + \Delta_i$. Due to not finding a suitable Lyapunov function to prove the stability of the system, the first definition of stability is used.

Let us define the output power tracking error of wind turbine i to be.

$$\tilde{P}_i = P_i - P_{VL} - \Delta_i, i = 1,..,N_w \tag{12}$$

In the next section there will be discussions and proofs about the stability of the wind turbine power regulation when following the modified local pursuit strategy. Also will be included are some remarks and lemmas based on the power formation stability proofs. The effect of rotor speed stability when using the modified local pursuit strategy will also be discussed. The consequences of rotor speed stability analysis on the rotor speed values and some comments on the kind of rotor speed values to expect based on these proofs will be also be discussed.

Lemma 1: As $t \to \infty$, the power output of wind turbine will asymptotically converge to its allocated value if $v_i > 0$. Under this guidance law, the power output is

$$P_i = \tilde{P}_i(t_0) e^{-\int_{t_0}^{tf} v_i(t)dt} + P_{VL} + \Delta_i, \ i = 1,..., N_w \tag{13}$$

Proof: It is proven in (Xu, Remeikas, and Pham 2013) that the error signal will asymptotically converge to zero as $t \to \infty$ if $v_i(t) > 0$. Thus the proof of this part of Lemma 1 is omitted.

According to Eq. (11) and Eq. (12), $\dot{\tilde{P}}_i = -v_i \tilde{P}_i$. Therefore,

$$\tilde{P}_i = \tilde{P}_i(t_0) e^{-\int_{t_0}^{tf} v_i(t)dt} \tag{14}$$

which leads to Eq. (13).

Equilibrium Point and Stability of Rotor Speed

In this section some analysis will be done to check the stability of the wind turbine rotor speed when the power output of the wind turbine is driven by the modified local pursuit strategy. It is important to do this to make sure using local pursuit strategy does not render the rotor speed unstable. Some analysis will also be done to determine the equilibrium point of the rotor speed thus obtained. The effects of perturbation and the limits of perturbation of the rotor speed equilibrium point, i.e. the attraction region, will also be analyzed.

Lemma 2: If the power generation follows Eq. (11), the equilibrium points of the rotor speed $\omega_{i,r}^{ss}$ are

$$\omega_{i,r}^{ss} = \left[-c_{i,2} \pm \sqrt{c_{i,2}^2 + 4c_{i,1}\left(P_{VL} + \Delta_i\right)} \right] / (2c_{1,i}),\ i = 1,...,N_w \tag{15}$$

in which the coefficients are defined in the following proof. Here a negative rotor speed represents the case that the rotor will spin in the opposite direction if allowed.

Proof: The rotor dynamics from Eq. (1) can be written as,

$$\dot{\omega}_{i,r} = \frac{\rho \pi R_i^2 V_i^3 C_p(\lambda_i, \beta_i)}{2J_{i,eq}\omega_{i,r}} - \frac{a_i n_{i,gb}^2 \omega_{i,r}}{J_{i,eq}} - \frac{b_i n_{i,gb}}{J_{i,eq}},\ i = 1,...,N_w \tag{16}$$

Let us define $c_{i,1} \triangleq a_i n_{i,gb}^2 > 0$ and $c_{i,2} \triangleq b_i n_{i,gb} < 0$, and also because $P_i = 0.5\rho\pi R_i^2 V_i^3 C_P(\lambda_i, \beta_i)$, the rotor dynamics can be rewritten as

$$\begin{aligned}\dot{\omega}_{i,r} &= \frac{1}{J_{i,eq}}\frac{P_i}{\omega_{i,r}} - \frac{c_{i,1}}{J_{i,eq}}\omega_{i,r} - \frac{c_{i,2}}{J_{i,eq}} \\ &= -\frac{c_{i,1}}{J_{i,eq}}\omega_{i,r} - \frac{c_{i,2}}{J_{i,eq}} + \frac{1}{J_{i,eq}\omega_{i,r}}\left(\tilde{P}_i(t_0)e^{-\int_{t_0}^{tf} v_i(t)dt} + P_{VL} + \Delta_i\right)\end{aligned} \tag{17}$$

Therefore, the equilibrium point $\omega_{r,eq}$ when $\dot{\omega}_i = 0$ gives,

$$\omega_{i,r}^{ss} = \left[-c_{2,i} \pm \sqrt{c_{2,i}^2 + 4c_{1,i}\left(\tilde{P}_i(t_0)e^{-\int_{t_0}^{tf} v_i(t)dt} + P_{VL} + \Delta_i\right)}\right] / \left(2c_{i,2}\right) \tag{18}$$

As $t \to \infty$, the steady state equilibrium point of the rotor speed is derived as Eq. (18).

In reality, a wind turbine may only have one equilibrium point according to its wind blade pitch angle installation.

The next lemma, will analyze the stability of the rotor speed equilibrium point with respect to perturbations to the stable equilibrium point state. In case of small perturbations of a system from its equilibrium point if it comes back to its equilibrium point the equilibrium point is considered to be asymptotically stable.

Lemma 3: If the power generation for each wind turbine follows the modified local pursuit equation (Eq. (11)), the equilibrium point of the rotor speed in Eq. (18) is asymptotically stable if the perturbation from its equilibrium point $\tilde{\omega}_{i,r}$ satisfies $\left|\tilde{\omega}_{i,r}\right| < \left|\omega_{i,r}^{ss}\right|$.

Proof: Let us assume the rotor speed is perturbed to be $\omega_{i,r} = \omega_{i,r}^{ss} + \tilde{\omega}_{i,r}$, where $\tilde{\omega}_{i,r}$ is the error around the equilibrium point. Then Eq. (18) can be rewritten as

$$\dot{\omega}_{i,r}^{ss} + \dot{\tilde{\omega}}_{i,r} = -\frac{c_{i,1}}{J_{i,eq}}\left(\omega_{i,r}^{ss} + \tilde{\omega}_{i,r}\right) - \frac{c_{i,2}}{J_{i,eq}} + \frac{1}{J_{i,eq}\left(\omega_{i,r}^{ss} + \tilde{\omega}_{i,r}\right)}\left(\tilde{P}_i(t_0)e^{-\int_{t_0}^{tf} v_i(t)dt} + P_{VL} + \Delta_i\right) \tag{19}$$

which can be simplified as

$$\begin{aligned}\dot{\omega}_{i,r}^{ss}+\dot{\tilde{\omega}}_{i,r} &= -\frac{c_{i,1}}{J_{i,eq}}\omega_{i,r}^{ss}-\frac{c_{i,1}}{J_{i,eq}}\tilde{\omega}_{i,r}-\frac{c_{i,2}}{J_{i,eq}} \\ &+\left[\frac{1}{\omega_{i,r}^{ss}}-\frac{\tilde{\omega}_{i,r}}{\omega_{i,r}^{ss}\left(\omega_{i,r}^{ss}+\tilde{\omega}_{i,r}\right)}\right]\frac{1}{J_{i,eq}}\left(\tilde{P}_i(t_0)e^{-\int_{t_0}^{tf}v_i(t)dt}+P_{VL}+\Delta_i\right)\end{aligned} \tag{20}$$

Remove the equilibrium part in Eq. (20), the error dynamics is derived to be

$$\dot{\tilde{\omega}}_{i,r}=-\frac{1}{\omega_{i,r}^{ss}\left(\omega_{i,r}^{ss}+\tilde{\omega}_{i,r}\right)J_{i,eq}}\left(\tilde{P}_i(t_0)e^{-\int_{t_0}^{tf}v_i(t)dt}+P_{VL}+\Delta_i\right)\tilde{\omega}_{i,r}-\frac{c_{i,1}}{J_{i,eq}}\tilde{\omega}_{i,r} \tag{21}$$

For any $v_i>0$,

$$\begin{aligned}\tilde{P}_i(t_0)e^{-\int_{t_0}^{tf}v_i(t)dt}+P_{VL}+\Delta_i &= \left(P_i(t_0)-P_{VL}-\Delta_i\right)e^{-\int_{t_0}^{tf}v_i(t)dt}+P_{VL}+\Delta_i \\ &= P_i(t_0)e^{-\int_{t_0}^{tf}v_i(t)dt}+\left(P_{VL}+\Delta_i\right)\left(1-e^{-\int_{t_0}^{tf}v_i(t)dt}\right)>0\end{aligned} \tag{22}$$

If $\left|\tilde{\omega}_{i,r}\right|<\left|\omega_{i,r}^{ss}\right|$, $\omega_{i,r}^{ss}\left(\omega_{i,r}^{ss}+\tilde{\omega}_{i,r}\right)>0$. Since $c_{i,1}>0$, the coefficients in both terms of the error dynamics are negative, which means the rotor speed error will decay to zero as $t\to\infty$, and the error is bounded by its initial error. Therefore, according to (Slotine, and Li 1991), the rotor speed equilibrium point is asymptotically stable.

In the following lemma we studied the effect of initial conditions on the on the rotor speed equilibrium point. In the case that the system's initial point is changed we are going study the behavior of the equilibrium point. In case of asymptotic stability the rotor speed will converge to its equilibrium point and it will considered 'attracting.' The region of attraction is determined in the next section.

Lemma 4: the regions of attraction for positive and negative $\omega_{i,r}^{ss}$ in Eq. (18) are $(0,\infty)$ and $(-\infty,0)$, respectively.

Proof: Let us define

$$f_i = -\left(c_{i,1}/J_{i,eq}\right)\omega_{i,r} - \left(c_{i,2}/J_{i,eq}\right) + \left(\tilde{P}_i(t_0)e^{-\int_{t_0}^{tf} v_i(t)dt} + P_{VL} + \Delta_i\right)/\left(J_i\omega_{i,r}\right) \tag{23}$$

There is a singular value at $\omega_{i,r} = 0$. For the positive $\omega_{r,eq}$ case, if $\omega_{i,r} = \omega_{i,r}^{ss} + \Delta_\omega$, Eq. (23) can be simplified as

$$\begin{aligned} f_i &= -\left(c_{i,1}/J_{i,eq}\right)\left(\omega_{i,r}^{ss} + \Delta_\omega\right) - \left(c_{i,2}/J_{i,eq}\right) + \left(\tilde{P}_i(t_0)e^{-\int_{t_0}^{tf} v_i(t)dt} + P_{VL} + \Delta_i\right)/\left[J_{i,eq}\left(\omega_{i,r}^{ss} + \Delta_\omega\right)\right] \\ &= -\left(c_{i,1}/J_{i,eq}\right)\Delta_\omega - \left[\left(\tilde{P}_i(t_0)e^{-\int_{t_0}^{tf} v_i(t)dt} + P_{VL} + \Delta_i\right)/J_{i,eq}\right]\frac{\Delta_\omega}{\left(\omega_{i,r}^{ss} + \Delta_\omega\right)\omega_{i,r}^{ss}} \end{aligned} \tag{24}$$

Note that the equilibrium condition is applied in deriving Eq. (24). Therefore, if $-\omega_{i,r}^{ss} < \Delta_\omega < 0$, $f_i > 0$ and $\omega_{i,r}$ will increase until it reaches $\omega_{i,r}^{ss}$. If $\Delta_\omega > 0$, $f_i < 0$ and $\omega_{i,r}$ will decrease until it reaches $\omega_{r,eq}$. Thus the region of attraction for the positive $\omega_{r,eq}$ will be $(0,\infty)$. Similarly, it can be proven that for the negative $\omega_{i,r}^{ss}$, the region of attraction is $(-\infty,0)$.

Based on Lemma 3, when the power output generated follows the modified local pursuit equation, if the initial rotor angular velocity is positive (negative), it will converge to the positive (negative) equilibrium point.

Based on Lemma 1 – Lemma 3 and Remark 1, if the power output follows Eq. (11), the rotor speed in the individual wind turbine will reach its equilibrium point depending on its initial condition, which is asymptotically stable.

Based on Eq. (13), $\tilde{P}_i(t_f) = \tilde{P}_i(t_0)e^{-\int_{t_0}^{t_f} v_i(t)dt}$. Thus

$$\ln\left[\tilde{P}_i(t_f)/\tilde{P}_i(t_0)\right] = -\int_{t_0}^{t_f} v_i(t)dt \tag{25}$$

This equation can provide you information on how fast roughly the power generated by wind turbine *i* will approach the allocated power.

It is worth noting the asymptotically stability of the equilibrium rotor speed assumes that the model is perfectly known and there is no sensor or actuator noises or uncertainties. When the noise and/or uncertainties cannot be neglected or the wind turbine is not perfectly modeled, the planning algorithm proposed here can be put in a receding horizon framework and the power generation in individual wind turbine will be re-planned at the beginning of each planning horizon.

In this section we have studied the stability properties of the wind turbine dynamic system. The difference here being that the power is now driven by the modified local pursuit strategy and the system was found to be asymptotically stable. The rotor speed equilibrium point equation was found and was also asymptotically stable. In the power planning it is expected that the initial conditions of the rotor speed could vary and this will not affect the equilibrium point and stability of the system. It was found based on the analysis also how quickly the power can be attained by the wind turbine following the local pursuit strategy and is mainly dependent on the speed control parameter value.

Dynamic Model Propagation

To solve the optimization problem for individual wind turbine listed in Section 3.A, we need to know the state and control variables at each instance. Since the input matrix of model Eq. (1) is non-square, instead of finding those variables through fast collocation methods such as those used in (Xu, Remeikas, and Pham 2013, Fahroo and Ross 2001), we will directly propagate the dynamic model here. The detailed steps involved are listed in the following algorithm.

Table 2 Algorithm 1 - Model propagation

Step 1	Based on the allocated power P_i for the i^{th} wind turbine using Eq. (11), the rotor power coefficient $C_P(\lambda_i, \beta_i)$ can be calculated using Eq. (2).
Step 2	The result from step 1 can be used to propagate the angular speed dynamics $\omega_{i,r}$ using the first equation in Eq. (1).
Step 3	The tip speed ratio is then calculated by $\lambda_i = \omega_{i,r} R_i / V_i$
Step 4	The tip speed ratio calculated in the previous step along with the known $C_P(\lambda_i, \beta_i)$ can help us reversely solve for the pitch angle β_i using Eqs. (4) and (5)
Step 5	The control variable (i.e. the reference pitch angle $\beta_{i,r}$) can be calculated using the derivative of β_i and the second equation in Eq. (1). The derivative of β_i can be approximated using the Euler scheme.
Step 6	The output variables, i.e. the thrust and torque on the rotor, can be calculated using Eq. (2). The tower deflection (z_i) is propagated using Eq. (7) based on the

calculated thrust F_i on the rotor.

Individual Wind Turbine Power Generation Optimization Algorithm

The optimization of the power generation in each wind turbine is shown in Algorithm 2 listed below. The "fmincon" solver in MATLAB is applied here. As proven in Lemma 3, the closed-loop system is asymptotically stable.

Table 3 Algorithm 2 – Power generation optimization

Step 1	Using the known virtual leader power P_{VL} and the allocated power bias Δ_i, guess the optimizable variable (i.e. the speed control parameter v_i) at each time node.
Step 2	The power P_i to be generated is propagated using the guessed v_i.
Step 3	Algorithm 1 is followed and the results are used in evaluating the performance index as defined in Eq. (8) and the equality and inequality constraints as described in Section 3.A.
Step 4	If the performance index does not converge to the minimum or a feasible solution, go back to Step 1. Else, the optimization is accomplished.

Wind turbines in a wind farm can be optimized using Algorithm 2 in a decentralized manner.

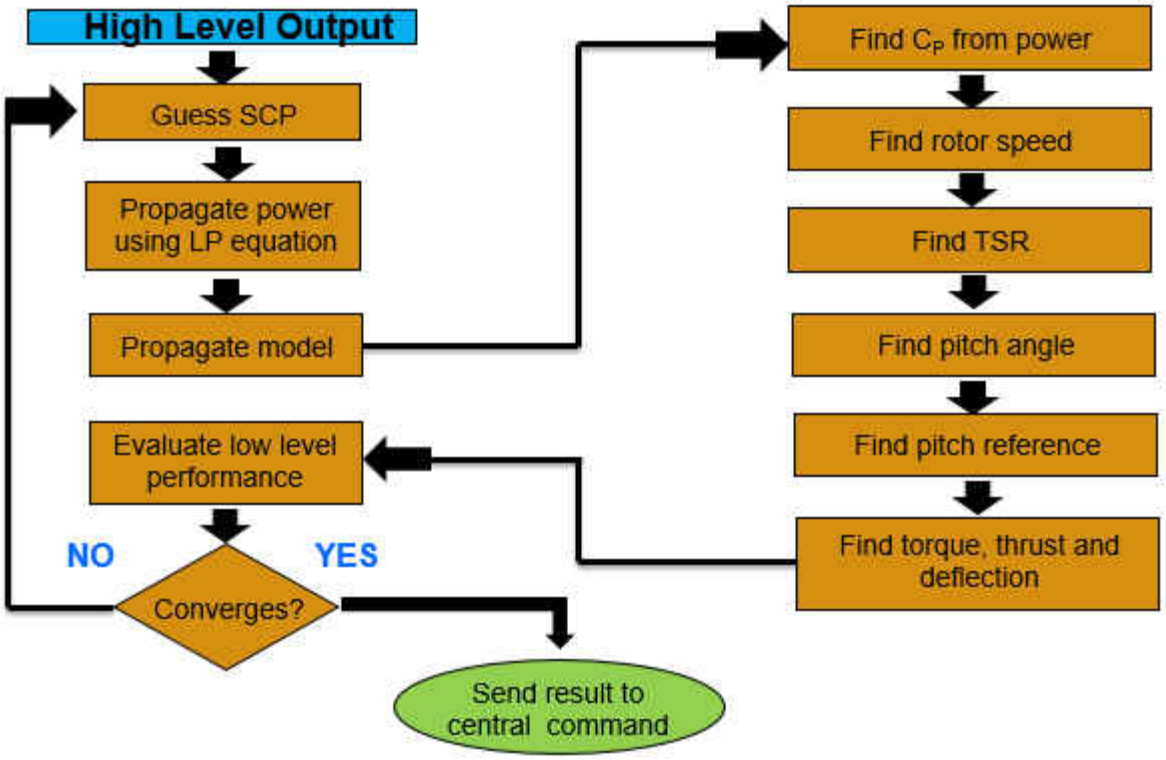

Figure 12 Lower level optimization algorithm

The lower level optimization algorithm is summarized in Fig. (12). The information coming from the upper level which includes, wind speeds at rows of wind turbines, the power to be allocated to each wind turbine in the wind farm, the initial wind turbine power, initial rotor speed (and pitch angle) and the virtual leader power. With these information in hand the lower level algorithm starts with setting SCP (γ) bounds and initial guess and uses the MALAB nonlinear optimization function 'fmincon' to guess an SCP value for the modified LP equation used for power propagation (Eq. (11)). Next the algorithm proceeds to propagate the wind turbine model, which forms the part of the 'fmincon' objective function. The steps are to find the coefficient of power from actual wind turbine power, finding the rotor speed from the model Eq. (1) for which the coefficient of power was just found and linearized torque parameters are already know for

the given wind speed region. With the rotor speed and wind speed known the tip speed ratio can be calculated. Knowing tip speed ratio and coefficient of power the pitch angle corresponding to that combination is extracted from Eq. (4), with pitch angle known the rate of change of pitch angle can be found. Knowing these information the algorithm inversely finds pitch reference angle, the rotor torque and rotor thrust using Eqs. (1) and (2). The performance index is then evaluated and if the constraints are met and the index cannot be further minimized the optimization comes to a stop otherwise it proceeds to guess a new SCP and repeat the process.

CHAPTER FIVE: COORDINATED POWER ALLOCATION IN A WIND FARM

Power Generation Allocation in Cooperative Level

The performance index in the cooperative level is given in Eq. (9). Expanding this performance index, we get

$$J = \left(\sum_{i=1}^{N_w} P_i \right)^2 - 2 \left(\sum_{i=1}^{N_w} P_i \right) P_{tot} + P_{tot}^2 \tag{26}$$

Minimizing Eq. (26) is equivalent to minimizing $J = \left(\sum_{i=1}^{N_w} P_i \right)^2 - 2 \left(\sum_{i=1}^{N_w} P_i \right) P_{tot}$. Expanding the first term in (26),

$$\left(\sum_{i=1}^{N_w} P_i \right)^2 = \left(\sum_{i=1}^{N_w} P_i \right) \left(\sum_{j=1}^{N_w} P_j \right) = \sum_{i=1}^{N_w} P_i \left(P_i + \sum_{i \neq j} P_j \right) = \sum_{i=1}^{N_w} P_i^2 + \sum_{i \neq j} P_j P_i \tag{27}$$

Therefore, the performance index can be written as the form of a quadratic programming as

$$J = \min_{\boldsymbol{P}} \frac{1}{2} \boldsymbol{P}^T H \boldsymbol{P} + f^T \boldsymbol{P} \tag{28}$$

where the optimizable parameters $\boldsymbol{P}^T = \left[P_1, P_2, ..., P_{N_w} \right]$ are the powers to be allocated. The matrices H and f are defined as

$$H = 2 \begin{bmatrix} 1 & 1 & .. \\ 1 & 1 & .. \\ .. & .. & .. \end{bmatrix}_{N_w \times N_w} \quad \text{and} \quad f = -2 P_{tot} \begin{bmatrix} 1 \\ 1 \\ .. \end{bmatrix}_{N_w \times 1} \tag{29}$$

The constraint in the optimal power allocation is $[\boldsymbol{P}_{\min}, \boldsymbol{P}_{\max}]$. To know the range of the available power for each wind turbine, the range of possible wind speed needs to be calculated. The

algorithm to calculate the lower and upper bounds of the available power $[\boldsymbol{P}_{\min}, \boldsymbol{P}_{\max}]$ is listed next as Algorithm 3.

Table 4 Algorithm 3 – Range of available power for each wind turbine

Step 1	Measure the upwind speed
Step 2	Calculate the coefficients of power (C_P) and thrust (C_T) ranges for the upwind turbines for all possible pitch angles at the optimal tip speed ratio.
Step 3	The information from Step 2 and the distances between the upwind and downwind rows of wind turbines are utilized to determine the range of wake velocities using the Jenson wake velocity equation in Eq. (6).
Step 4	Using the result from Step 3 to compute the range of available power for all possible pitch angles.
Step 5	Repeat Step 2 and Step 3 for any more downwind rows.

The MATLAB quadratic programming solver "quadprog" is used to solve the formulated power allocation problem (Eqs. 28 and 29 and $\boldsymbol{P} \in [\boldsymbol{P}_{\min}, \boldsymbol{P}_{\max}]$). The algorithm used to optimally allocate the power to each wind turbine is summarized in the following table.

Table 5 Algorithm 4 – Quadratic programming for coordinated power allocation

Step 1	Receive the total wind farm power demand (P_{tot})
Step 2	Follow Algorithm 3 to find $\boldsymbol{P}_{\min}$ and $\boldsymbol{P}_{\max}$
Step 3	Solve the formulated quadratic programming problem (Eqs. 28 and 29 and $\boldsymbol{P} \in [\boldsymbol{P}_{\min}, \boldsymbol{P}_{\max}]$)

Step 5	Compute the virtual leader power ($P_{VL} = P_{tot} / N_w$ and $\dot{P}_{VL} = 0$)
Step 6	Send the allocated power ($P_i = P_{VL} + \Delta_i$), virtual leader power (P_{VL}), and bias information (Δ_i) to Algorithm 2 for lower level optimization. This step is decentralized.

Coordinated Power Allocation and Planning Algorithm

Algorithms 1 through 4 are put together in Algorithm 5 as the overall power allocation and optimal power planning algorithm for a wind farm.

Table 6 Algorithm 5 – Summary of the algorithm

Step 1	The grid sends a total desired power output (P_{tot}) in the beginning of each planning horizon.
Step 2	Algorithm 4 (including Algorithm 3) is used to find P_{VL}, P_i and Δ_i in the cooperative level, which will be sent to individual wind turbine (centralized).
Step 3	Algorithm 2 (including Algorithm 1) is used to find the optimized v_i and the optimal reference pitch angle $\beta_{i,r}$ (decentralized).
Step 4	Send the overall operation and power production information back to the central computer. Individual wind turbine will execute the $\beta_{i,r}$ command.

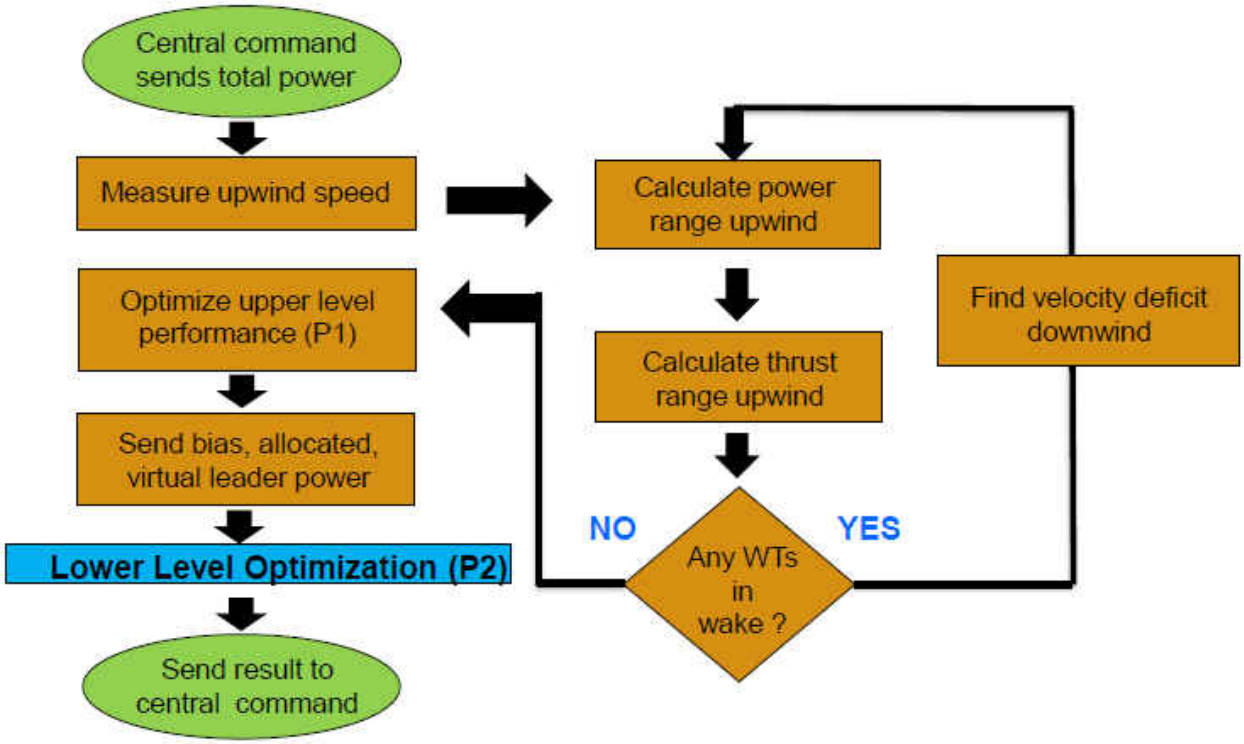

Figure 13 Higher level optimization algorithm

The upper level optimization algorithm is summarized in Fig. (13). The wind farm measurements provide the downwind distances between wind turbine rows. The wind speed at the front row of wind turbines is known before the start of upper level optimization. For the simulation an initial power and initial rotor speed value are set for the wind turbines, and as a result of this an initial pitch angle is also set as the three are a function of each other for a given wind speed. In a real wind farm these values would be known based operational data. The upper level algorithm is also responsible for populating the wind turbine constants and properties as mentioned in Table. 1, it also defines the non dimensionalization constants, the time horizon, the propagation step size, time node size and length of time node and virtual leader wind turbine rate of change of power. For a given total wind farm power requirement, the algorithm defines a

virtual leader power value. For current work this value was chosen to be a constant and average of the total power demand by the number of wind turbines. Knowing the upwind speed and distances, the algorithm finds the minimum and maximum power (power bounds) for each wind turbine in the first row and then does similar calculation for subsequent wind turbine rows. To find the ranges the algorithm varies the pitch angle values for an optimal tip speed ratio, which for the present wind turbine is around 7.55. For finding the wind speeds at subsequent rows the wind turbine uses the Jensen wake model presented in Eq. (6). With the power bounds (upper and lower bounds) of the optimization problem, the algorithm uses 'quadprog' solver to minimize the equivalent performance index shown in Eq. (28) and find the power to be allocated to each wind turbine. The results are then sent to the lower level for individual wind turbine optimization.

CHAPTER SIX: SIMULATION AND DISCUSSION

Simulation Settings

The constrained nonlinear programming problem in Algorithm 2 is solved using the MATLAB "fmincon" function (Choosing a solver, 2015); while the constrained linear quadratic programming problem in Algorithm 4 is solved by the "quadprog" function (Choosing a solver, 2015). The properties of the wind turbine are adopted from (Jonkman, Butterfield, Musial, and Scott 2009) as shown in Table 1. It is worth mentioning that although all the wind turbines in the simulated wind farm are assumed to be the same, non-homogenous dynamics models can be used in the proposed cooperative control algorithm.

In the upper level part of the algorithm initial power for wind turbines is set to 0 MW and a rotor speed of roughly 8 RPM is chosen to be the initial value. The initial pitch angle is related to the tip speed ratio(a function of wind speed and rotor speed) and power setting and is calculated using these two initial values. These are arbitrary values and in real scenario will be different. The initial guess for pitch angle when inversely finding pitch angle in Algorithm 1, is 20 deg.

The tolerances for the constraints and optimizable parameter (SCP) were set to 10^{-3} while function evaluations are set to 10^{-1}. For "quadprog" all options were kept at default setting. The upper and lower bounds of the optimizable parameter (i.e. the speed control parameter) are set to be between 4 and 8. It is crucial for this number to stay positive all the time. The initial guess for SCP was set to be 7.5. For extracting the coefficient of power and thrust values from NREL data, the cubic interpolation was used in MATLAB. The constraints on the rotor speed, torque, and force are limited by $1\,rpm \le \omega_r \le 15\,rpm$, $0 \le T \le 4.6\times10^{6}\ N\cdot m$, and $0 \le F \le 10^{6}\ N$,

respectively (Jonkman, Butterfield, Musial, and Scott 2009). The maximum tower deflection ($z_{\max}$) constraint is kept at 5% of the tower height. As one case, the weights in performance index Eq. (8) are set to $W_1 = 1$, $W_2 = 0$, and $W_3 = 0$. All the quantities in the optimization are non-dimensionalized to help the optimization convergence.

Individual Wind Turbine Optimization

Wind turbines in wind farm can experience a variety of wind speeds and different power output requirements, in this section these variations in wind speeds and power requirement were simulated, also since wind turbines in a wind farm could be operating at different initial power setting which in turn implies different initial rotor speed and pitch angle settings one scenario was simulated for varied initial power. Therefore, three scenarios are simulated to test the robustness of Algorithm 2, i.e. the power planning optimization of individual wind turbine: A) varying wind speed, B) varying allocated power, and C) varying initial power condition. During the planning horizon, it is presumed that the wind speed remains constant.

1) Case A: Varying Wind Speed

The table below summarizes the optimization results of varying wind speeds for a fixed set of allocated and initial wind turbine power, as well as an invariant virtual leader power.

The obtained steady state values for rotor speed, pitch angle, rotor torque, and rotor thrust are in agreement with those in similar scenarios on a 5 MW NREL wind turbine in (Jonkman, Butterfield, Musial, and Scott 2009). The minor differences in those performances are due to fact that the generator torque values (i.e. the values of *a* and *b*) chosen for the simulation are different from the data in NREL. Our strategy is to tune the generator torque to keep the tip speed ratio

between 7 and 8 near the optimal tip speed ratio of 7.55 (Jonkman, Butterfield, Musial, and Scott 2009).

Optimum solutions are able to be attained in reasonable time as shown in Table 7, ranging between 1.8 and 2.8 seconds.

Table 7 Case A – Varying wind speed

Case	V (m/s)	P (MW)	P_{VL} (MW)	P_0 (MW)	CPU time (sec)	β^{ss} (deg)	ω^{ss} (rpm)	T^{ss} (MN-m)	F^{ss} (MN)
A1	11.40	1.00	1.00	0.50	2.81	17.92	13.28	1.20	0.19
A2	10.00	1.00	1.00	0.50	1.84	16.07	11.71	0.90	0.14
A3	9.00	1.00	1.00	0.50	1.80	13.76	10.66	0.68	0.11
A4	8.00	1.00	1.00	0.50	1.83	9.93	9.59	0.51	0.08
A5	7.00	1.00	1.00	0.50	1.82	3.00	8.88	1.21	0.23

The following figures shows the time history of the wind turbine state and output variables for those five varying wind speed cases. In Fig. (15 – (16), the torque and thrust force are within the limit. The rotor speed (Fig. (17)) is stabilized at its equilibrium point based on its power output and blade pitch angle. In all the cases, the power generation reaches its allocated number 1 MW (Fig. (14). The pitch angle (Fig. (18) follows well with the commanded reference pitch angle (Fig. (19). It is worth noting that all five cases have different initial pitch angle due to the fact that there are only two independent variables among the initial power, initial blade pitch angle, and initial rotor speed settings.

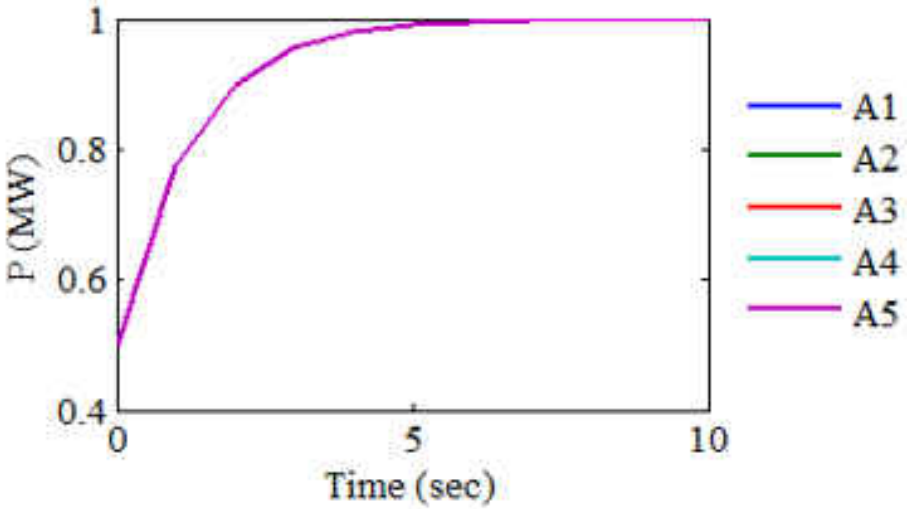

Figure 14 Case A power results

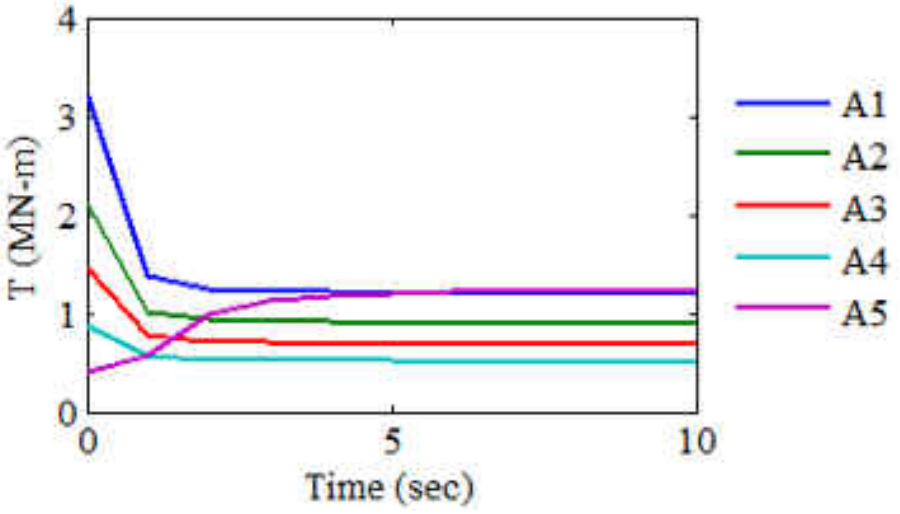

Figure 15 Case A torque results

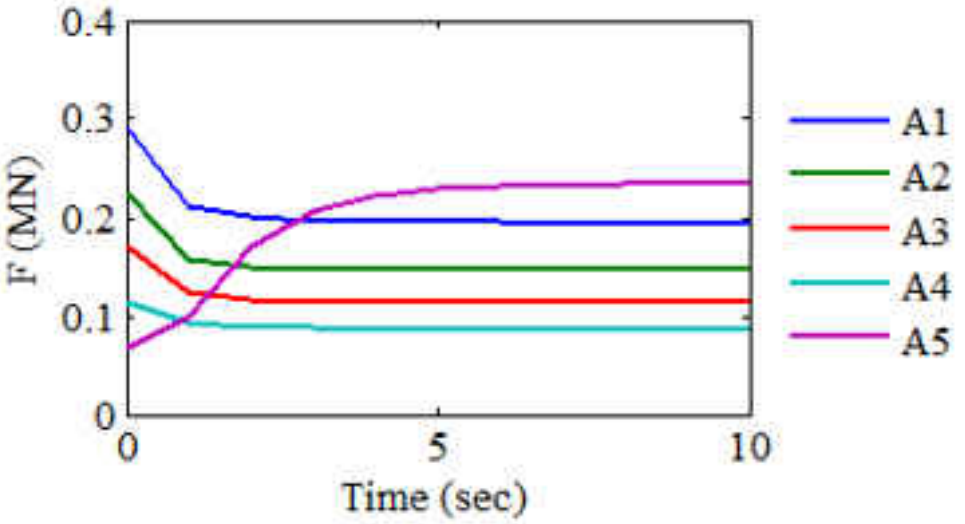

Figure 16 Case A thrust results

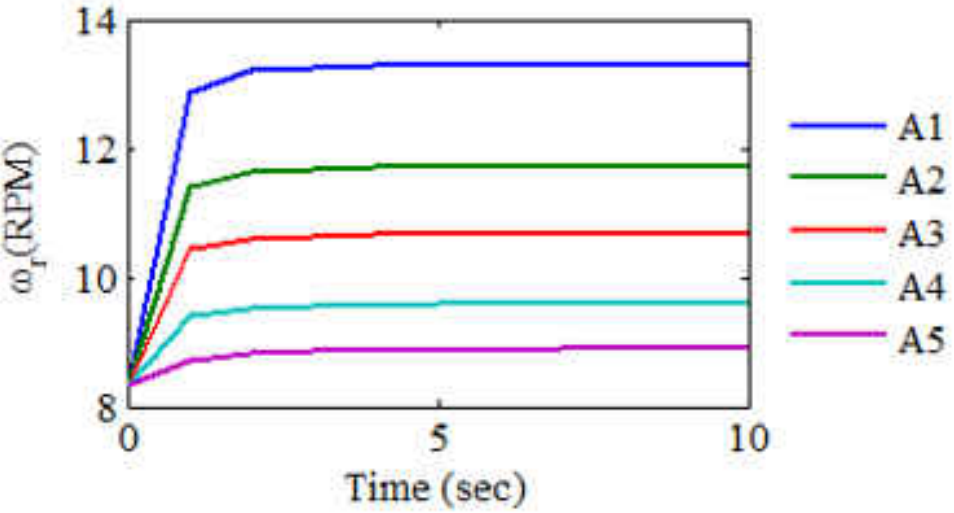

Figure 17 Case A rotor speed results

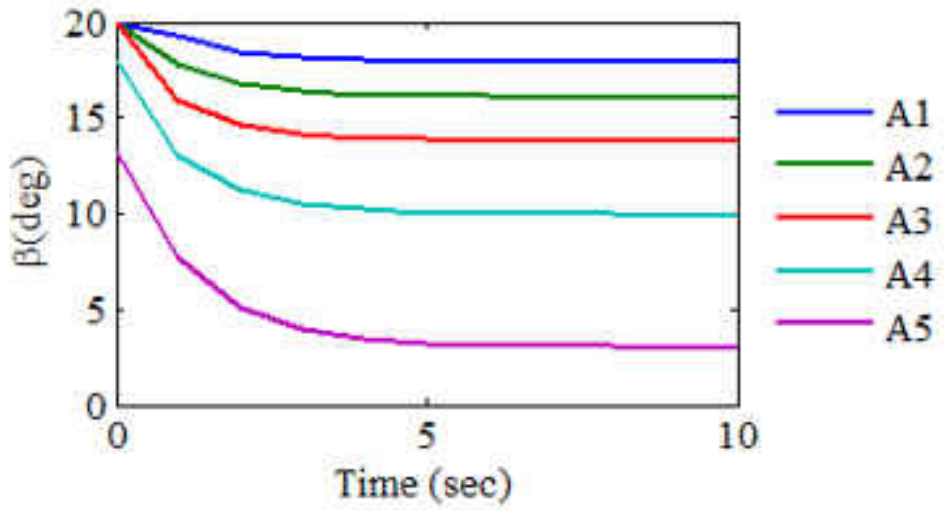

Figure 18 Case A pitch angle results

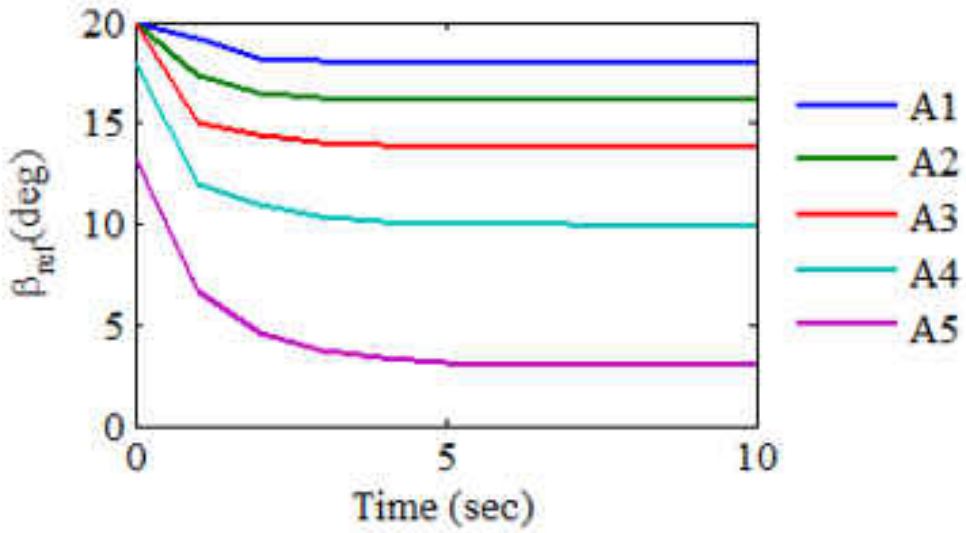

Figure 19 Case A pitch reference angle results

2) Case B: Varying Allocated Power

For the cases in Table 8, the allocated power is changing and the wind speed is kept constant. As expected with an increase in power demand, the pitch angle decreases. The maximum tower deflection, force, and thrust experienced by the turbine are increasing in a general trend. The CPU time is between 1.79 and 2.82 seconds. The rotor speed is maintained at its equilibrium point according to its power output, wind speed, and blade pitch angle.

Table 8 Case B – Varying allocated power

Case	V (m/s)	P (MW)	P_{VL} (MW)	P_0 (MW)	CPU time (sec)	β^{ss} (deg)	ω^{ss} (rpm)	T^{ss} (MN-m)	F^{ss} (MN)
B1	11.40	1.00	1.00	0.50	2.82	17.92	13.28	1.20	0.19
B2	11.40	2.00	1.00	0.50	1.83	13.70	13.73	1.00	0.17
B3	11.40	3.00	1.00	0.50	1.82	9.32	14.16	0.82	0.15
B4	11.40	4.00	1.00	0.50	1.79	4.67	14.57	2.72	0.49
B5	11.40	5.00	1.00	0.50	1.83	1.24	14.95	3.37	0.74

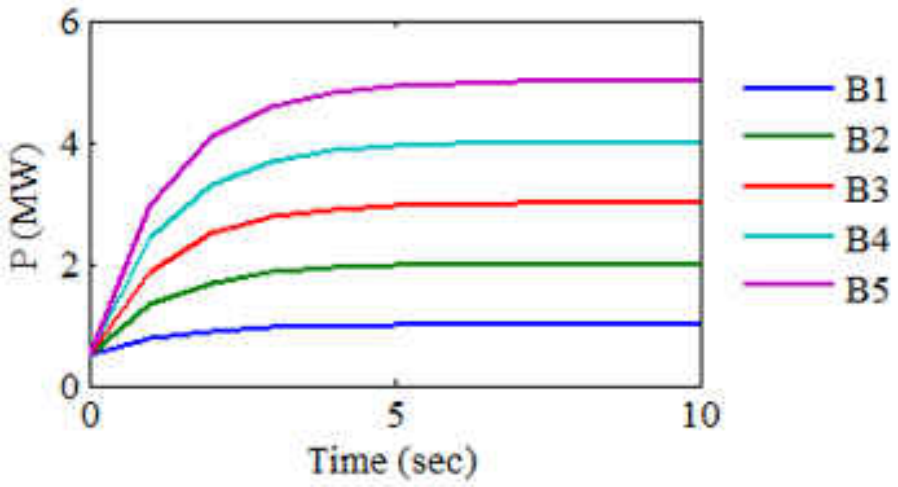

Figure 20 Case B power results

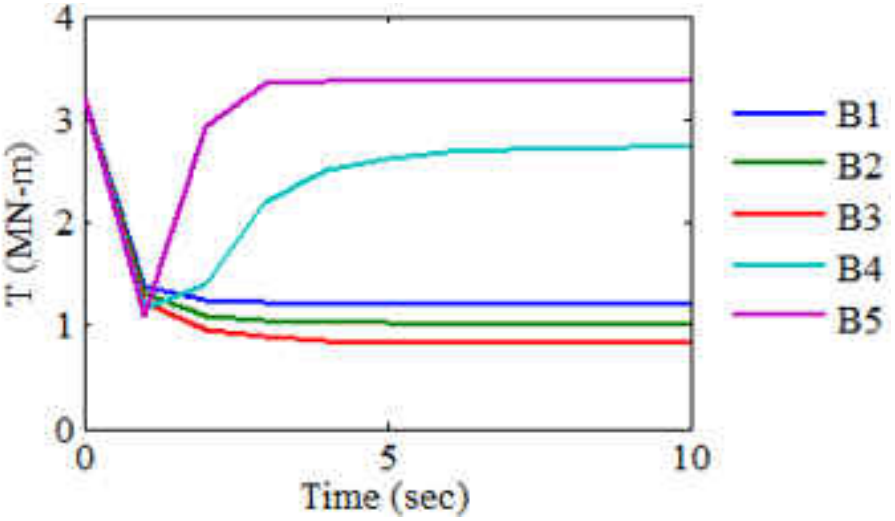

Figure 21 Case B torque results

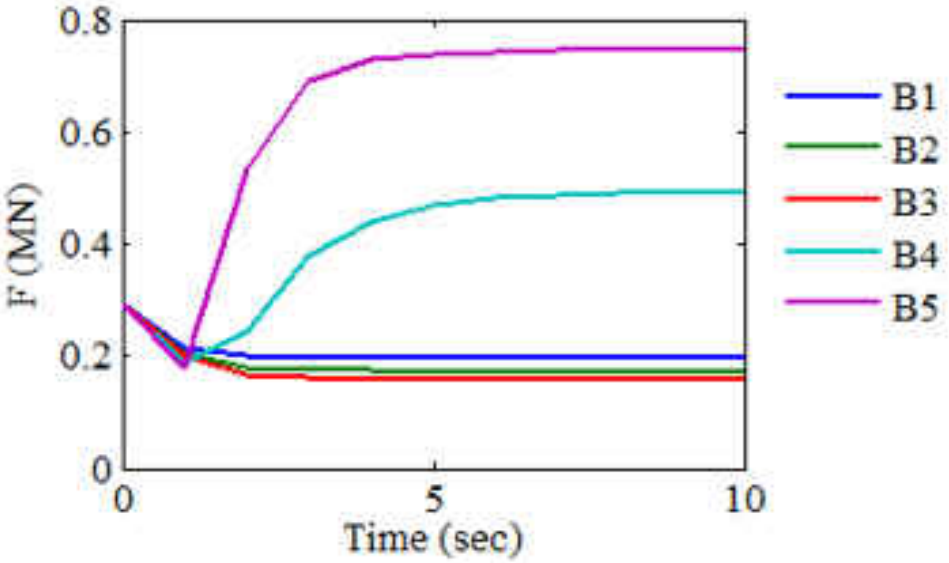

Figure 22 Case B thrust results

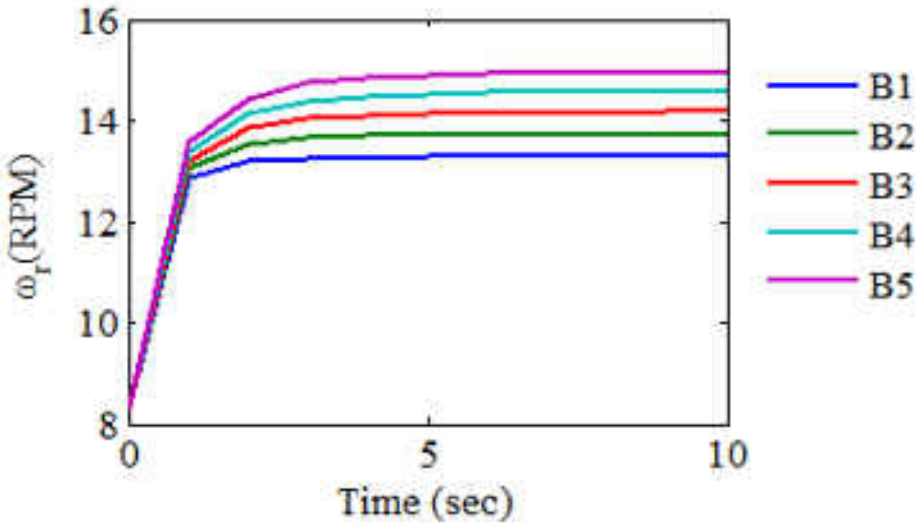

Figure 23 Case B rotor speed results

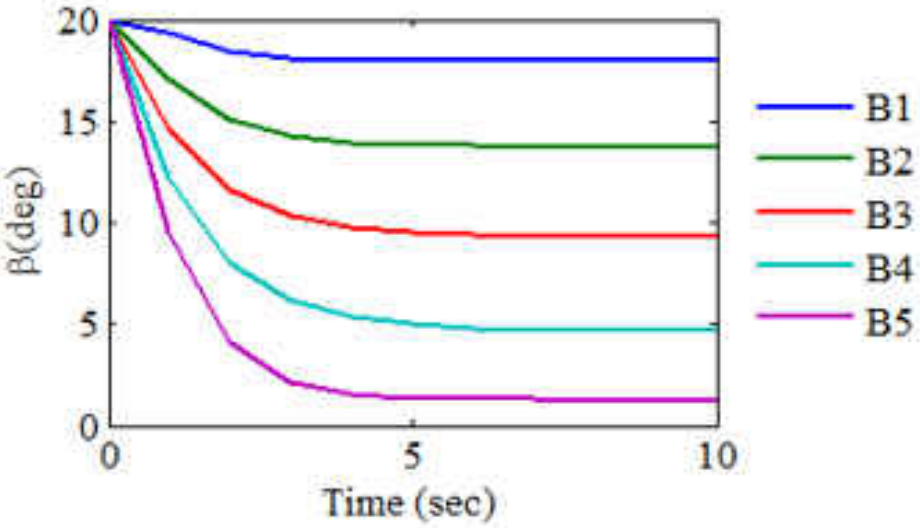

Figure 24 Case B pitch angle results

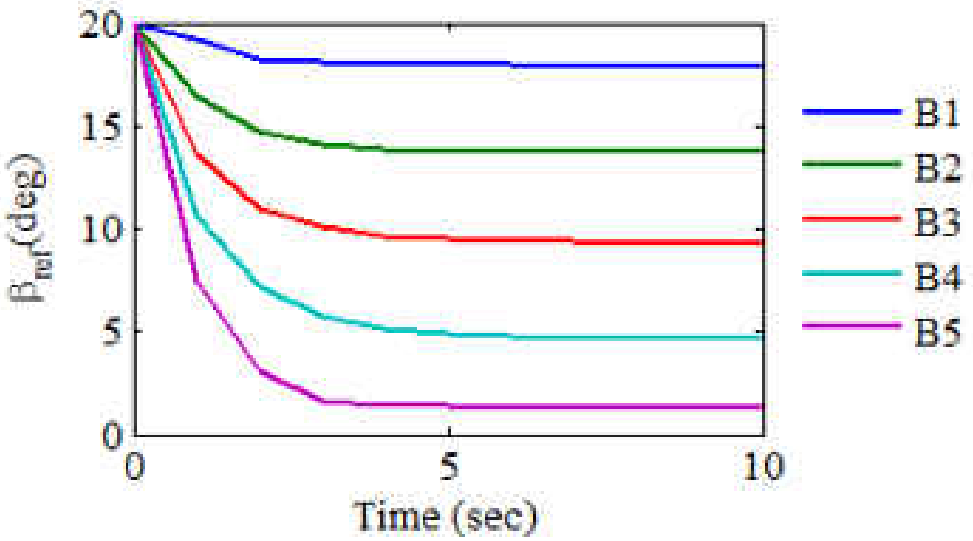

Figure 25 Case B pitch reference angle results

3) Case C: Varying Initial Power Condition

For all five C cases, the initial power condition is varied, while the wind speed and the allocated power are kept at the rated value. For the same commanded power at the same (rated) wind speed, the steady state values for all 5 cases achieve the same value as expected. The maximum tower deflection is different due to its different initial power output, which affects the transient stage of the power generation; however it is within the limit.

Table 9 Case C – Varying initial power condition

Case	V (m/s)	P (MW)	P_{VL} (MW)	P_0 (MW)	CPU time (sec)	β^{ss} (deg)	ω^{ss} (rpm)	T^{ss} (MN-m)	F^{ss} (MN)
C1	11.40	5.00	1.00	0.00	2.99	1.25	14.95	3.37	0.74
C2	11.40	5.00	1.00	1.00	1.86	1.25	14.95	3.37	0.74
C3	11.40	5.00	1.00	2.00	1.82	1.24	14.95	3.37	0.74

Case	V (m/s)	P (MW)	P_{VL} (MW)	P_0 (MW)	CPU time (sec)	β^{ss} (deg)	ω^{ss} (rpm)	T^{ss} (MN-m)	F^{ss} (MN)
C4	11.40	5.00	1.00	3.00	1.80	1.24	14.95	3.37	0.74
C5	11.40	5.00	1.00	4.00	1.78	1.24	14.95	3.37	0.74

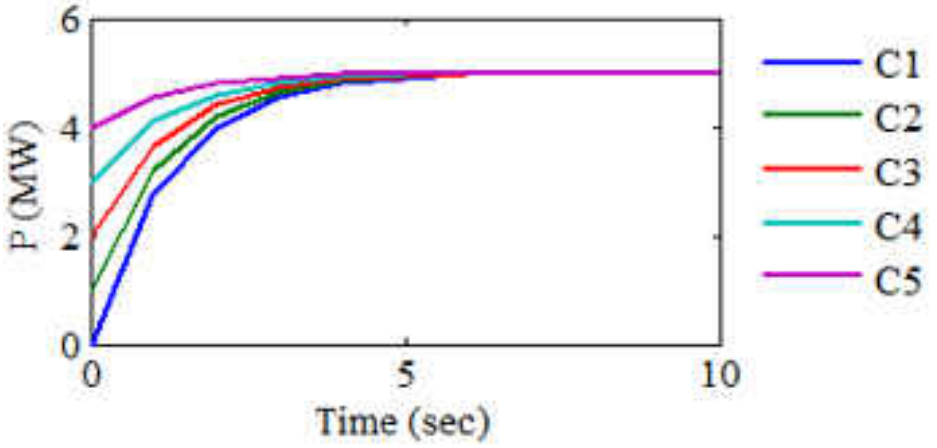

Figure 26 Case C power results

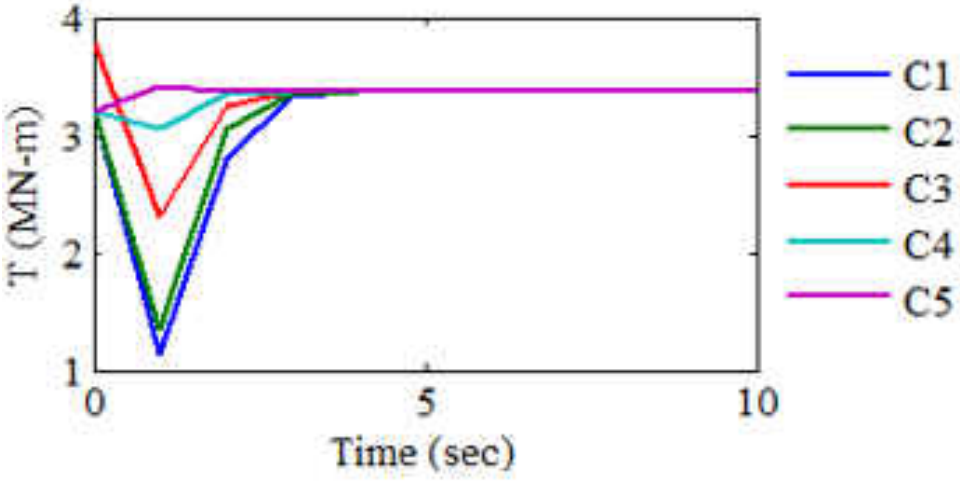

Figure 27 Case C torque results

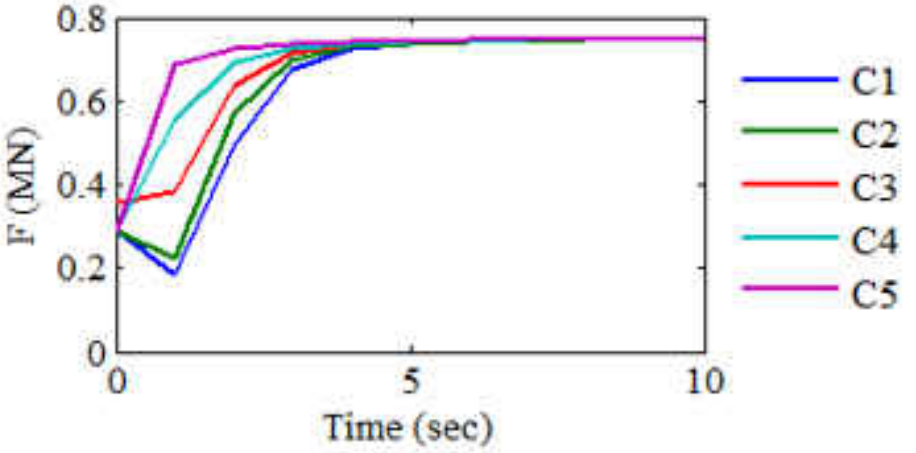

Figure 28 Case C thrust results

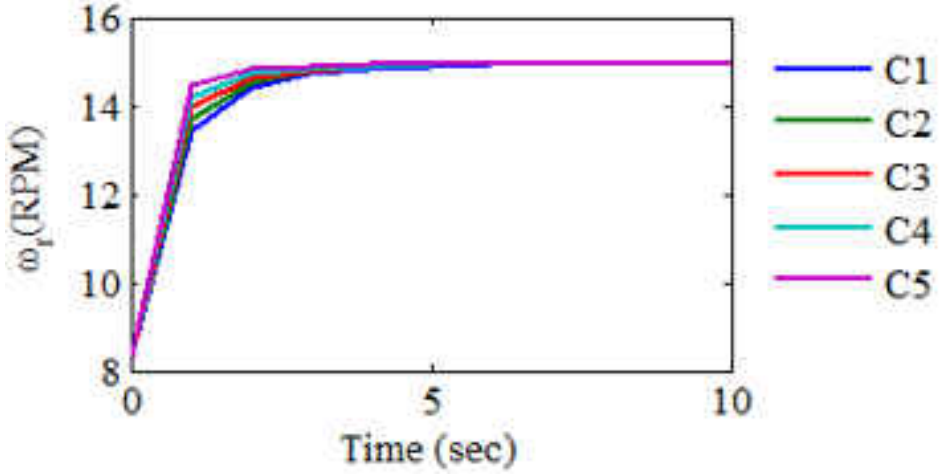

Figure 29 Case C rotor speed results

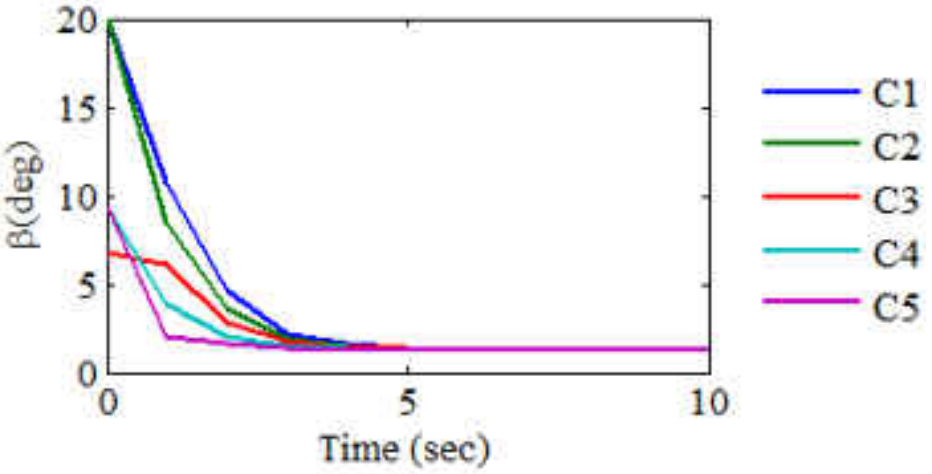

Figure 30 Case C pitch angle results

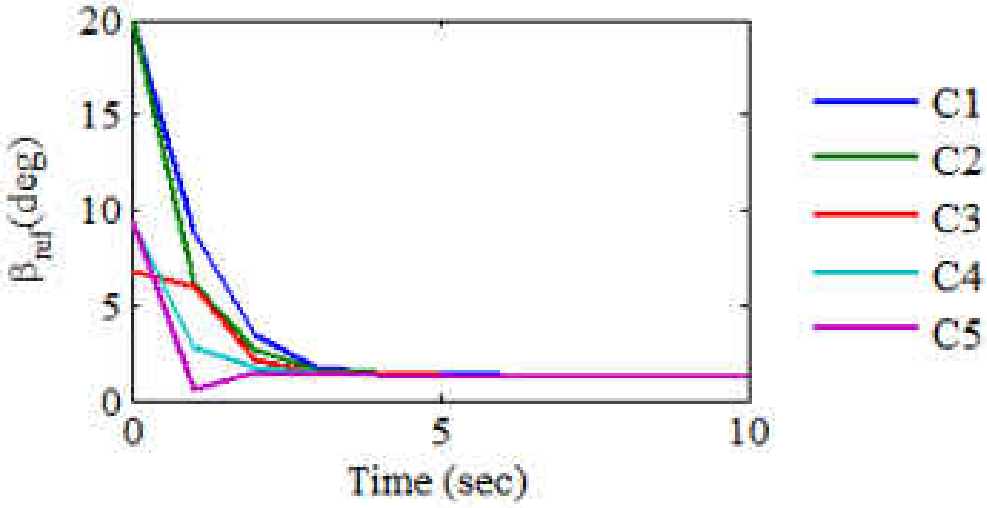

Figure 31 Case C pitch angle reference results

Coordinated Wind Turbine Optimization

The overall cooperative optimal power planning algorithm (Algorithm 5) is tested on three offshore wind farms with different sizes. The individual wind turbine's performance is akin to that shown in the earlier section and the constraints are met.

4) Case D: A 2x2 Wind Farm Array

In this case, an array consisting of 4 wind turbine array is selected (Fig. (32)). The distance between each row of wind turbines is 504 m. A total power demand of 10 MW is requested from the farm. A rated wind speed of 11.4 m/s is available at the first row of wind turbines. Following Algorithm 5 and subsequent algorithms within it, the downwind wind speed at the second row is 10.13 m/s and the CPU time used in allocating the power to the wind turbines is 0.33 sec. The individual level algorithm is then minimizing the performance index in Eq. (8) and determines the pitch angle references for the individual wind turbines.

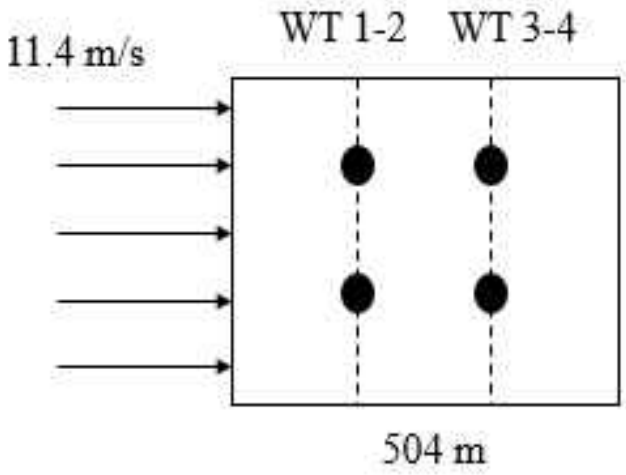

Figure 32 A 2x2 wind farm configuration

Table 10 2x2 Wind farm results

WT	V (m/s)	P (MW)	CPU Time (sec)	β_{ss} (deg)	$\omega_{r,ss}$ (RPM)	T_{ss} (MN-m)	F_{ss} (MN)
1	11.40	2.62	1.83	11.05	14.00	0.89	0.16
2	11.40	2.64	1.92	11.00	14.00	0.88	0.16
3	10.13	2.29	0.94	7.49	13.86	0.77	0.16
4	10.13	2.43	1.81	7.11	13.92	1.09	0.21

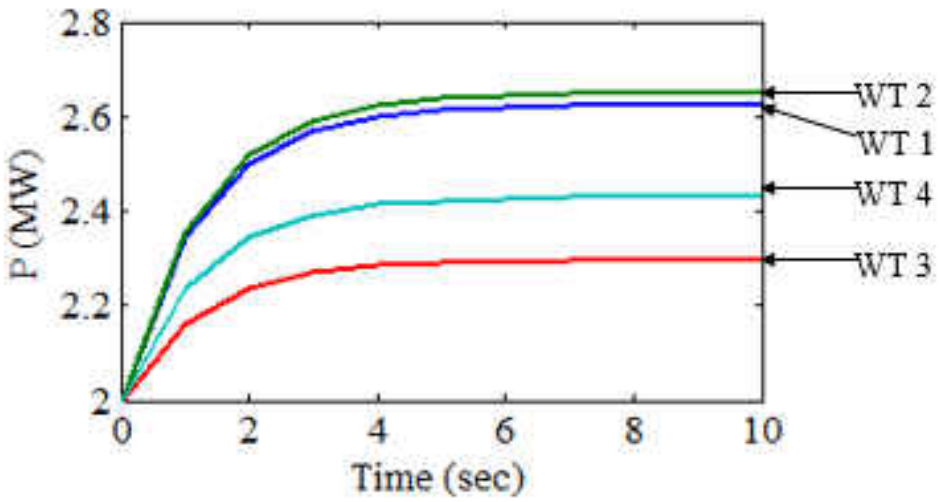

Figure 33 Power plots 2x2 case

The power output trend for the wind turbines can be seen in Fig. (33). The wind turbines were able to meet their power allocated values within the planning time and stay within the calculated bounds.

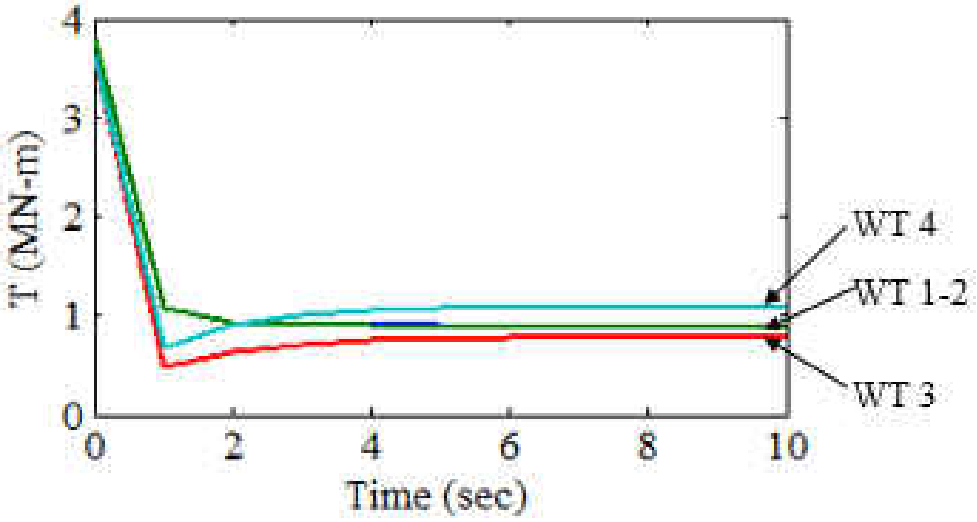

Figure 34 Torque plots of 2x2 case

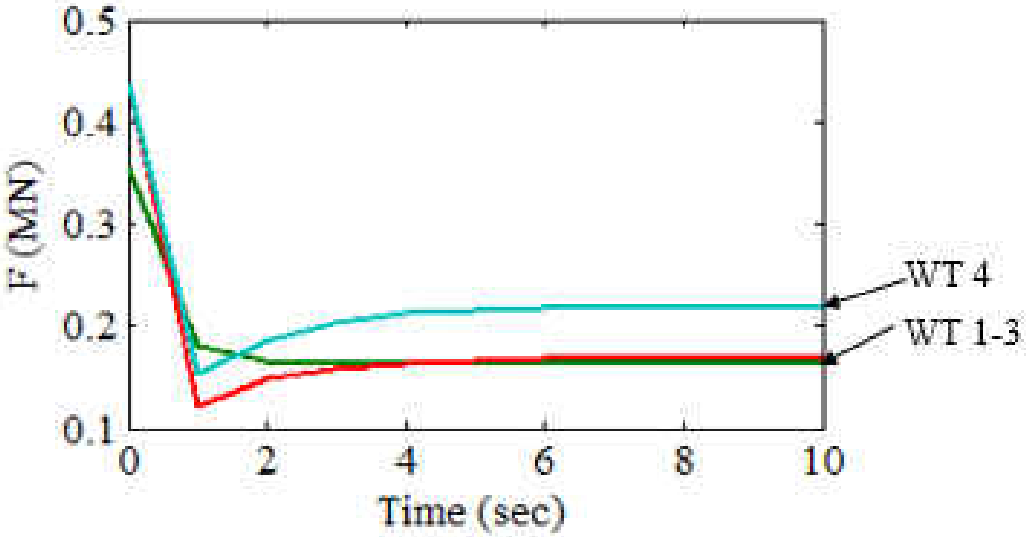

Figure 35 Thrust plots of 2x2 case

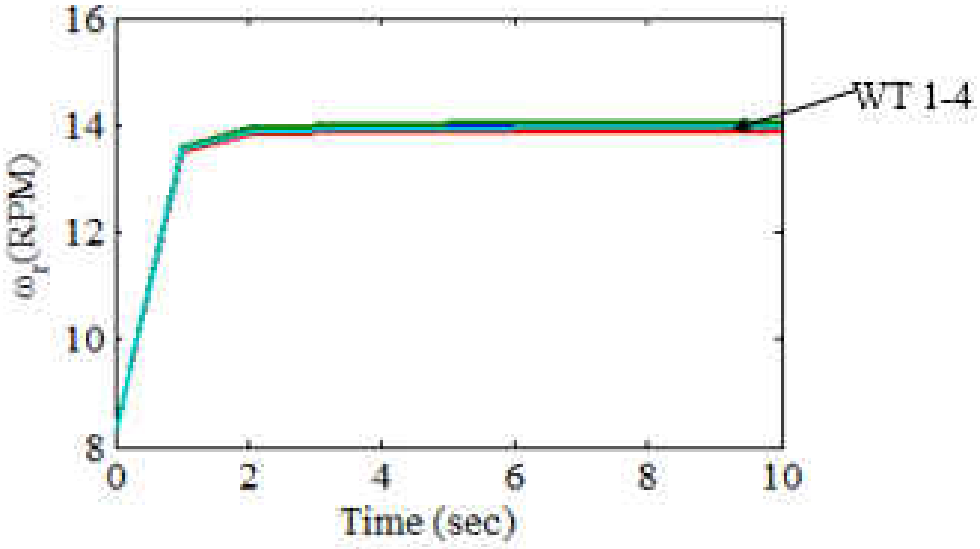

Figure 36 Rotor speed plots of 2x2 case

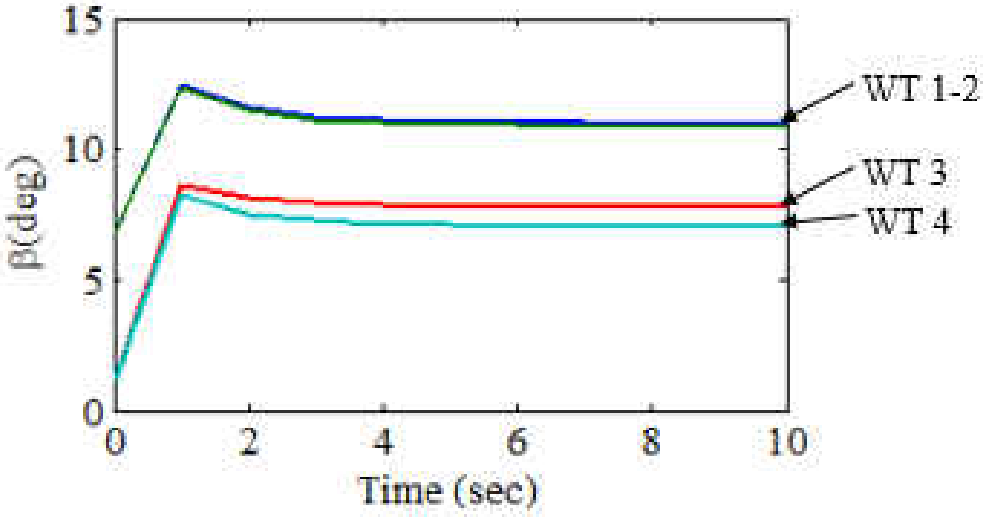

Figure 37 Pitch angle plots of 2x2 case

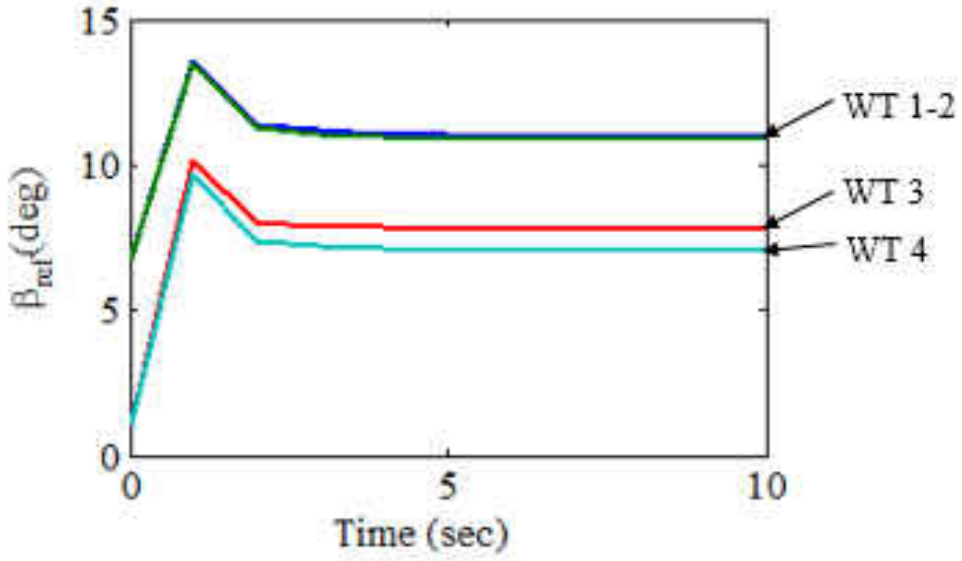

Figure 38 Pitch reference angle plots of 2x2 case

The sum of the power allocated to wind turbines was able to match with the total power demand, and the wind turbines were able to reach their allocated power. All the constraints remained within limits. The CPU time for the optimization was under 2 seconds for all the wind turbines. For simulation of the 2x2 case additional weights were added to the upper and lower bound power allocation values, which explains the differences between individual wind turbine power for the same upwind speed at the rows. The initial pitch angle is a function of the initial power, wind speed and initial rotor speed selected and that is evident from the pitch angle plots shown in Fig. (37). For the purpose of simulation initial power and rotor speed selected for all wind turbines was the same, in a real wind farm this information may be different for each wind turbines and will be known.

5) Case E: A 4x4 Wind Farm Array

In the second case a bigger array is used (Fig. 39). Here again a rated wind speed of 11.4 m/s is available in the first row of wind turbines. For a total power demand of 30 MW, the cooperative

level algorithm could rapidly allocate power to each wind turbines. The calculated velocities at the 2nd, 3rd and 4th rows are 9.83 m/s, 8.74 m/s, 7.54 m/s. The CPU time of the cooperative power allocation is 0.35 sec.

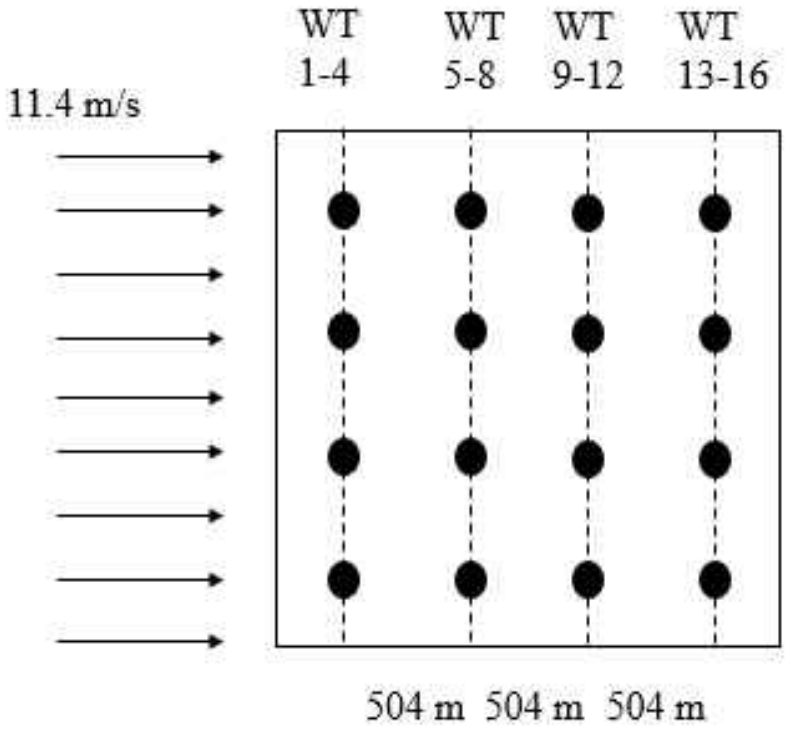

Figure 39 A 4x4 wind farm configuration

Table 11 4x4 Wind farm results

WT	V (m/s)	P (MW)	CPU Time (sec)	β_{ss} (deg)	$\omega_{r,ss}$ (RPM)	T_{ss} (MN-m)	F_{ss} (MN)
1	11.4	3.10	2.98	8.82	14.21	0.90	0.17
2	11.4	3.10	2.06	8.82	14.21	0.90	0.17
3	11.4	3.10	2.06	8.82	14.21	0.90	0.17
4	11.4	3.10	2.04	8.82	14.21	0.90	0.17
5	9.83	1.67	2.02	11.11	12.03	0.68	0.12
6	9.83	1.67	2.02	11.11	12.03	0.68	0.12
7	9.83	1.67	2.02	11.11	12.03	0.68	0.12
8	9.83	1.67	2.02	11.11	12.03	0.68	0.12
9	8.74	1.42	2.04	8.64	10.87	0.60	0.11
10	8.74	1.42	2.06	8.64	10.87	0.60	0.11
11	8.74	1.42	2.02	8.64	10.87	0.60	0.11
12	8.74	1.42	2.03	8.64	10.87	0.60	0.11
13	7.54	1.29	2.04	2.58	9.74	1.42	0.28
14	7.54	1.29	2.04	2.58	9.74	1.42	0.28
15	7.54	1.29	2.06	2.58	9.74	1.42	0.28
16	7.54	1.29	2.04	2.58	9.74	1.42	0.28

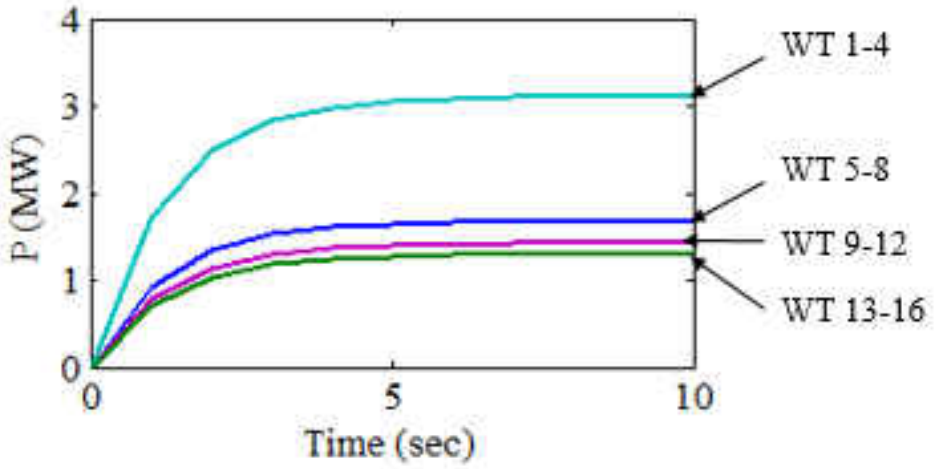

Figure 40 Power plots of 4x4 case

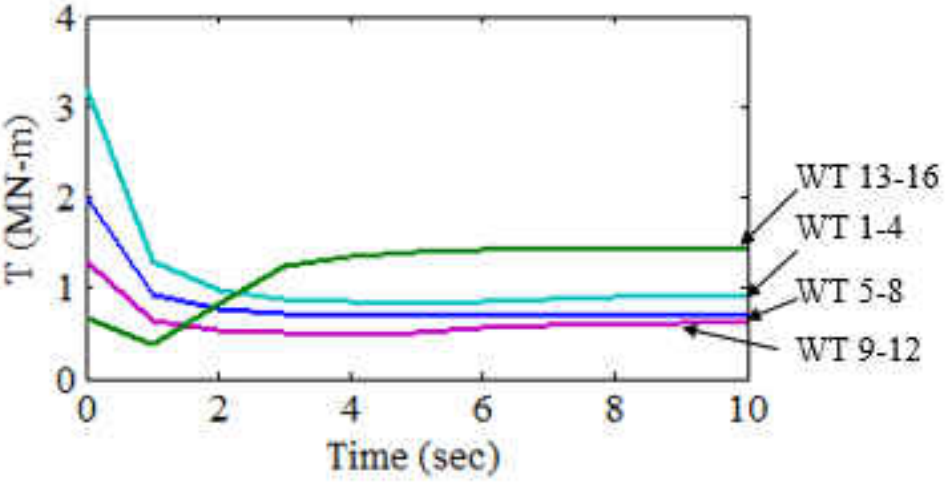

Figure 41 Torque plots of 4x4 case

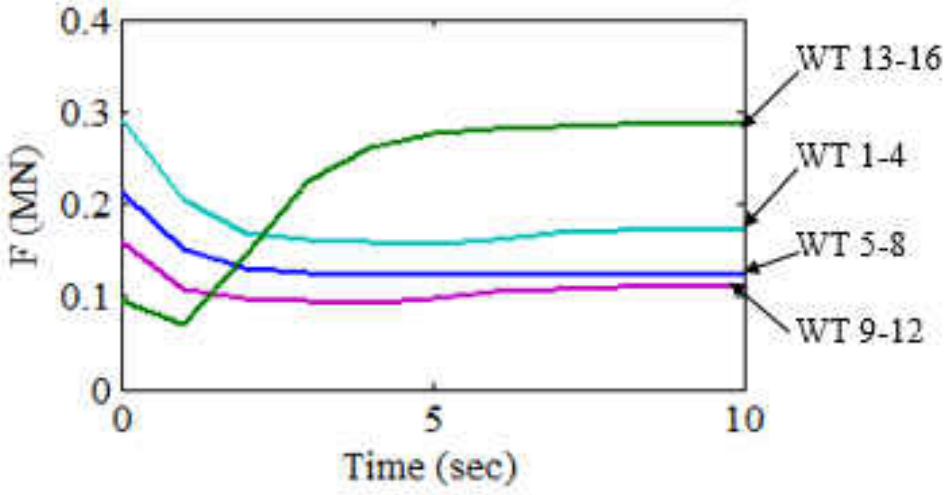

Figure 42 Thrust plots of 4x4 case

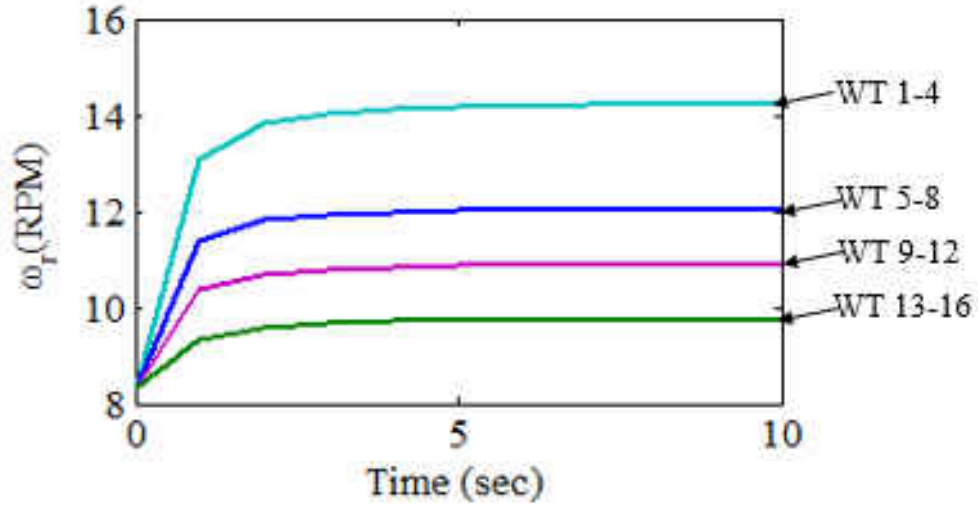

Figure 43 Rotor speed plots of 4x4 case

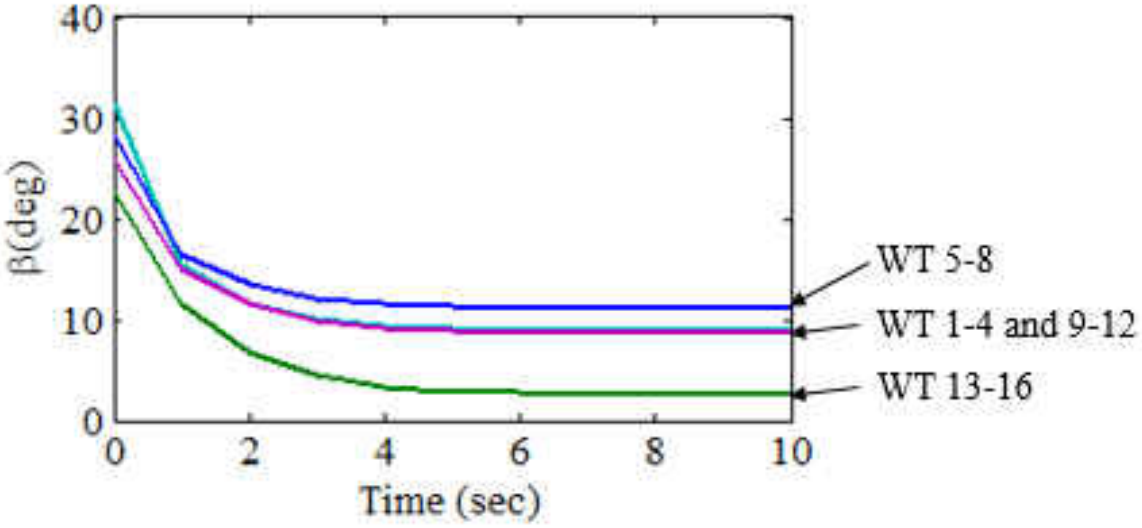

Figure 44 Pitch angle plots of 4x4 case

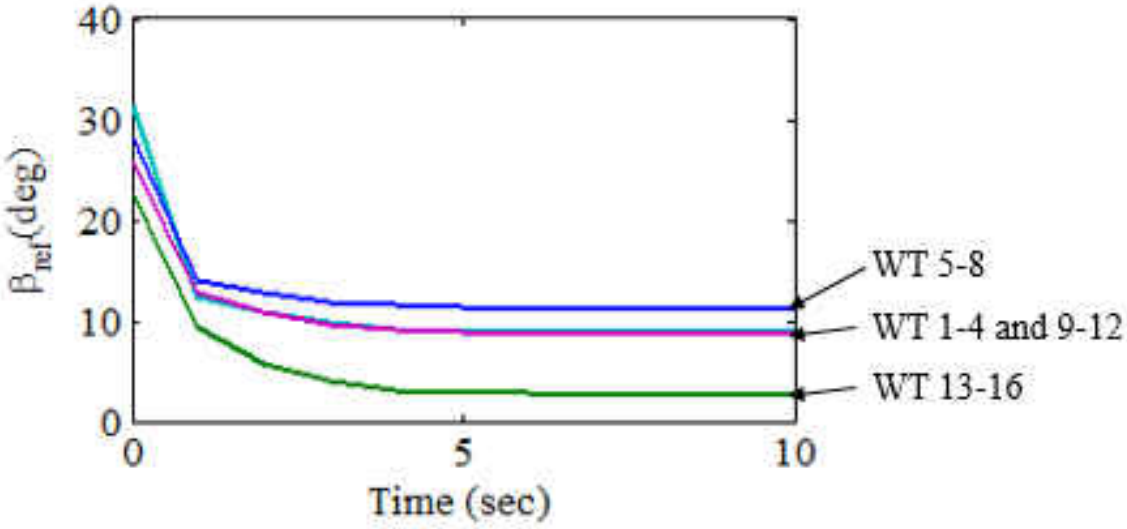

Figure 45 Pitch reference angle plots of 4x4 case

The total power demand was met by the sum of the allocated power and the wind turbines were able to reach their allocated power fairly quickly. All the model constraints were satisfied during the optimization. The allocated power was the same for wind turbines in each row, or the

same power was allocated for the same upwind speeds. The pitch angle setting for the power outputs were in agreement with wind turbine operation data. The wind turbines receiving less wind had to pitch more to produce the allocated power, also in agreement were the torque and thrust experienced by the rotor for those settings. The CPU time taken for the optimization of all cases remained under 3 seconds.

6) Case F: A 5x5 Wind Farm Array

For similar upwind conditions, in the case with 25 wind turbines (Fig. (46)), the total power demand from the wind farm is 45 MW. The calculated wind speeds based on the cooperative level algorithm at the downwind rows 2, 3, 4 and 5 are 9.84 m/s, 8.75 m/s, 7.55 m/s, and 5.91 m/s, respectively. The CPU time of the cooperative power allocation is 0.36 sec.

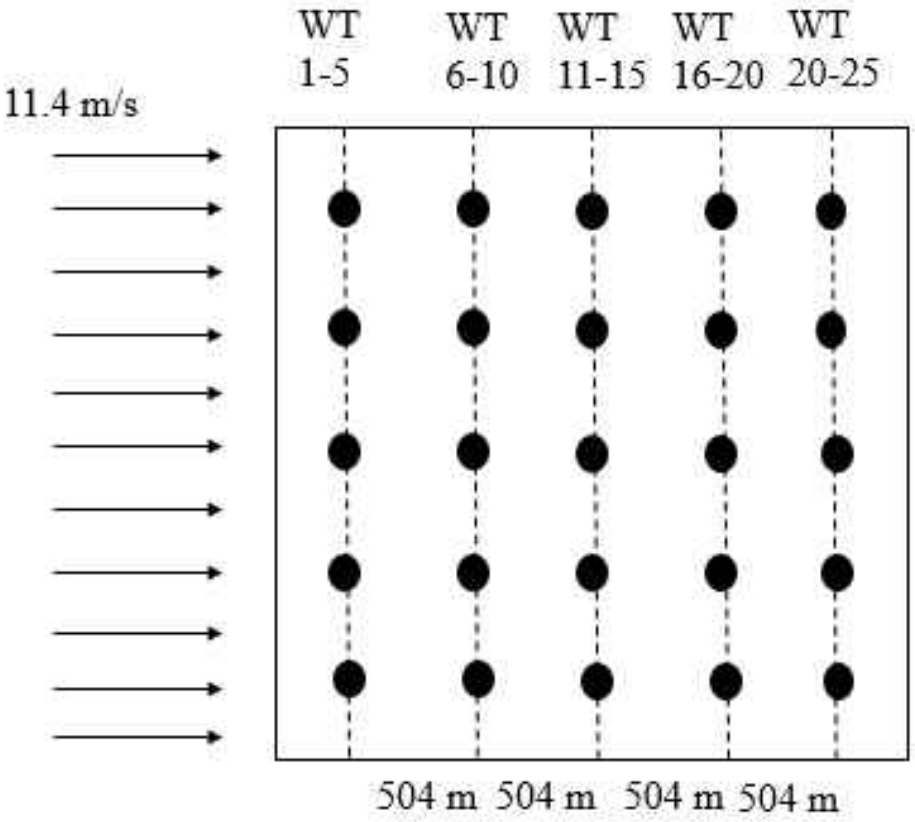

Figure 46 A 5x5 wind farm array

Table 12 4x4 Wind farm results

WT	V (m/s)	P (MW)	CPU Time (sec)	β_{ss} (deg)	$\omega_{r,ss}$ (RPM)	T_{ss} (MN-m)	F_{ss} (MN)
1	11.40	3.21	2.98	8.38	14.30	1.15	0.21
2	11.40	3.21	2.07	8.38	14.30	1.15	0.21
3	11.40	3.21	2.05	8.38	14.30	1.15	0.21
4	11.40	3.21	2.04	8.38	14.30	1.15	0.21

WT	V (m/s)	P (MW)	CPU Time (sec)	β_{ss} (deg)	$\omega_{r,ss}$ (RPM)	T_{ss} (MN-m)	F_{ss} (MN)
5	11.40	3.21	2.06	8.38	14.30	1.15	0.21
6	9.84	1.68	2.02	11.10	12.00	0.68	0.12
7	9.84	1.68	2.05	11.10	12.00	0.68	0.12
8	9.84	1.68	2.04	11.10	12.00	0.68	0.12
9	9.84	1.68	2.07	11.10	12.00	0.68	0.12
10	9.84	1.68	2.02	11.10	12.00	0.68	0.12
11	8.75	1.47	2.02	8.19	10.90	0.75	0.13
12	8.75	1.47	2.04	8.19	10.90	0.75	0.13
13	8.75	1.47	2.06	8.19	10.90	0.75	0.13
14	8.75	1.47	2.03	8.19	10.90	0.75	0.13
15	8.75	1.47	2.06	8.19	10.90	0.75	0.13
16	7.55	1.36	2.06	1.84	9.78	1.48	0.31
17	7.55	1.36	2.07	1.84	9.78	1.48	0.31
18	7.55	1.36	2.06	1.84	9.78	1.48	0.31
19	7.55	1.36	2.10	1.84	9.78	1.48	0.31
20	7.55	1.36	2.15	1.84	9.78	1.48	0.31
21	5.91	1.29	2.16	0.00	7.60	0.93	0.22
22	5.91	1.29	2.10	0.00	7.60	0.93	0.22
23	5.91	1.29	2.10	0.00	7.60	0.93	0.22

WT	V (m/s)	P (MW)	CPU Time (sec)	β_{ss} (deg)	$\omega_{r,ss}$ (RPM)	T_{ss} (MN-m)	F_{ss} (MN)
24	5.91	1.29	2.10	0.00	7.60	0.93	0.22
25	5.91	1.29	2.10	0.00	7.60	0.93	0.22

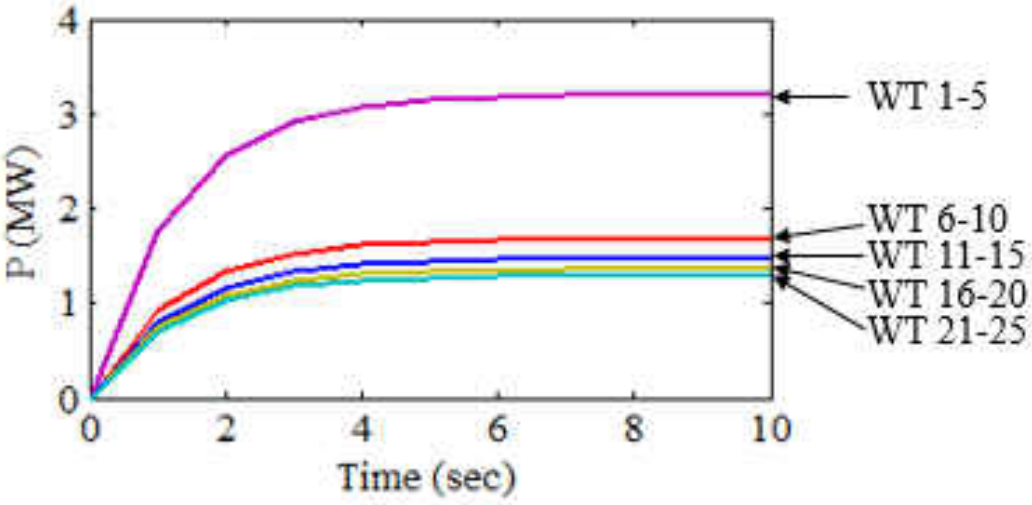

Figure 47 Power plots of 5x5 case

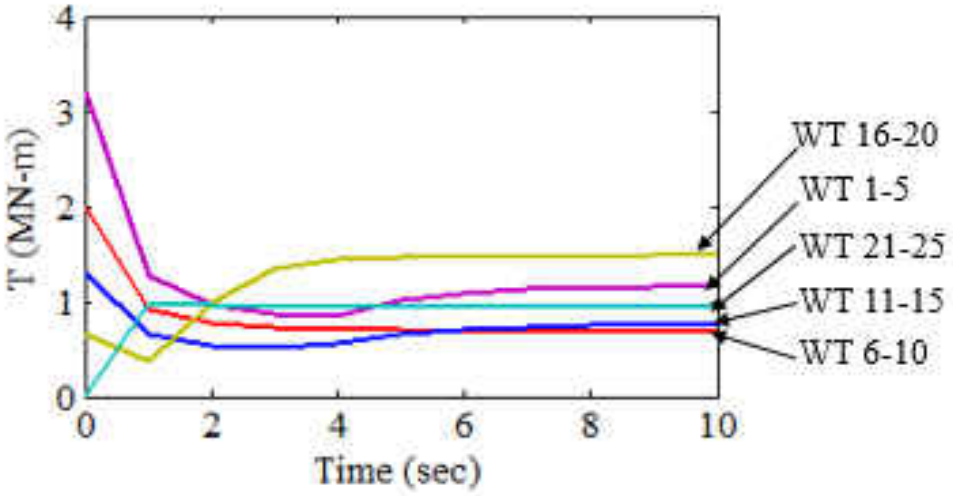

Figure 48 Torque plots of 5x5 case

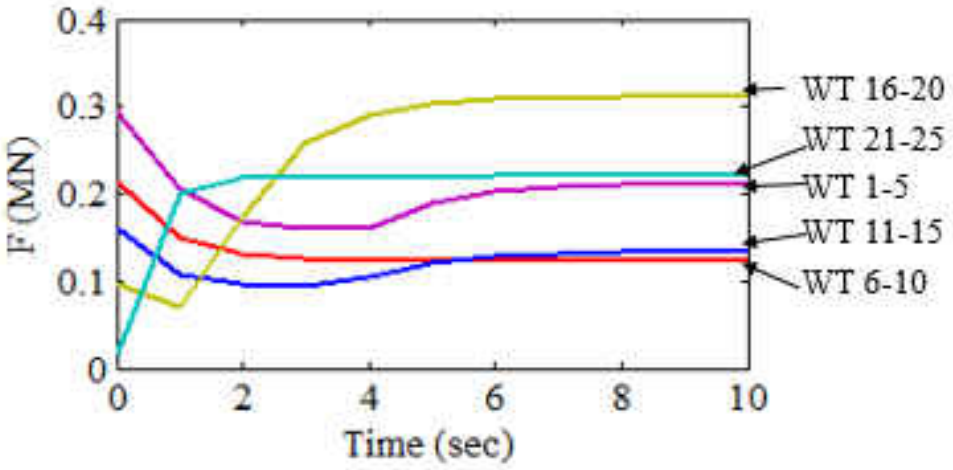

Figure 49 Thrust plots of 5x5 case

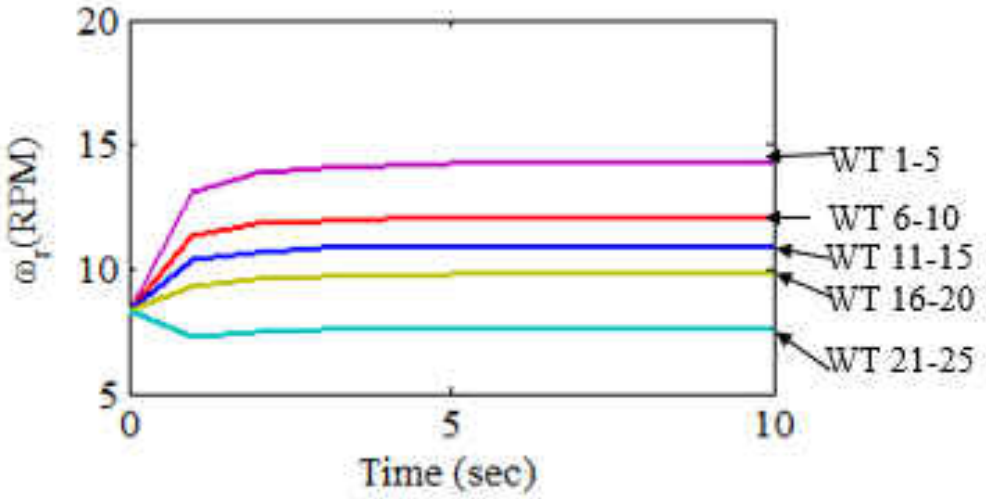

Figure 50 Rotor speed plots of 5x5 case

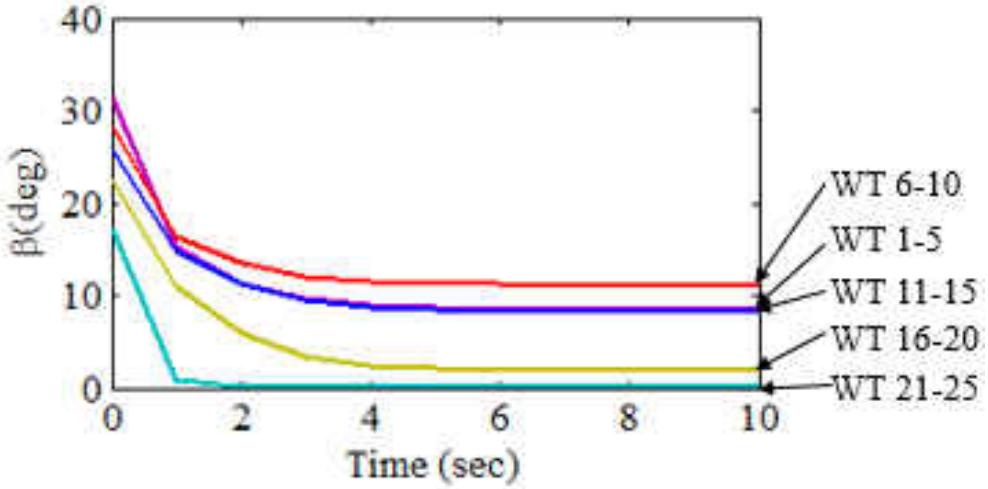

Figure 51 Pitch angle plots of 5x5 case

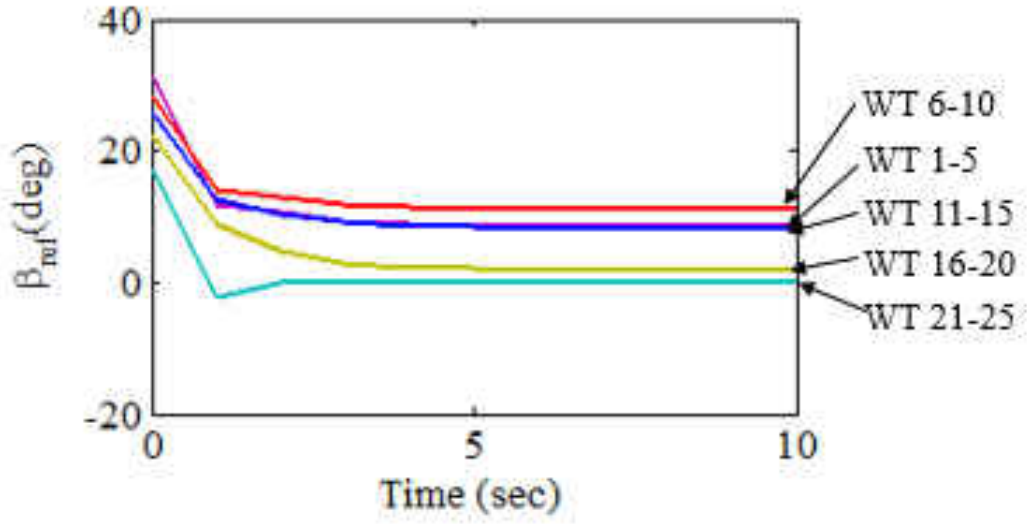

Figure 52 Pitch reference angle plots of 5x5 case

The total power demand was able to be met by the wind turbines in the wind farm. The CPU time taken for each wind turbine to carry out optimization remained under 3 seconds. The wind turbine experiencing the same upwind conditions were allocated the same power by the upper level algorithm. All the turbines were able to respect the local level constraints during the propagation. The back row turbines experiencing low wind speeds were operating at the maximum pitch angle settings to produce the allocated power. The increase in wind farm size had negligible effect in the CPU time for optimization.

The table below demonstrates the scalability of the cooperative power planning algorithm proposed in this paper. For an increase in the farm size, the computational cost remains at a similar level. The CPU time for the cooperative level only increases slightly from 0.33 seconds to 0.36 seconds. The CPU time increase for the individual level is relatively very low. The power allocation and planning optimization in a typical wind farm is at most 0.1 Hz (Knudsen, Bak, and Svenstrup 2014); therefore the CPU time achieved here meets the need. Furthermore,

with a more efficient C programming solver, the CPU time is expected to be much lower. The algorithm was also able to successfully handle all the coupled and uncoupled constraints imposed on it. The wind turbine models used in the algorithm are replaceable and do not depend on the chosen models. The data used for the model nonlinear power and thrust coefficients were taken from NREL and reflect a real wind turbine operational data.

Table 13 CPU time for three wind farms with different size

Wind farm configuration	2x2 array	4x4 array	5x5 array
Cooperative level			
CPU time (sec)	0.33	0.35	0.36
Performance index	0	0	0
Individual level			
Minimum CPU time (sec)	0.94	2.02	2.02
Maximum CPU time (sec)	1.94	2.98	2.98
Overall			
CPU time (sec)	2.27	3.33	3.34

CHAPTER SEVEN: CONCLUSION AND FUTUREWORK

Conclusion

With an increase in wind energy's contribution to power demands there is also increase in sizes of wind farms. This requires a scalable algorithm with low computational cost for allocating power to wind turbines in a wind farm to meet its demanded power. As wind turbines in a wind farm interact with each other aerodynamically this effects the power production of wind turbines. This also requires an algorithm which takes into account the effect of aerodynamic interaction.

In this dissertation, a new, hierarchical method for cooperative control of wind turbines in a wind farm is presented. The method presented has two levels, cooperative and individual. The power allocation among wind turbines is obtained by solving a formulated quadratic constrained programming problem taking into account coupled and uncoupled constraints. The coupled constraints comes from the aerodynamic interaction in the form of wind speed loss and the uncoupled constraints are the individual wind turbine limits on operation. The local pursuit strategy is customized for each wind turbine to optimally track the allocated power command taking into account realistic wind turbine constraints. A nonlinear wind turbine model was used for the work and offshore wind turbine data was used for simulation. The algorithm was simulated for three different sizes of offshore wind farm.

The algorithm was validated with simulations done for wind farm arrays of differing sizes, with a desired power demand and experiencing rated wind speeds. The lower level algorithm was also tested for its robustness for different initial power settings, wind speed availability and power demand.

The benefits of the algorithms are found to be as follows: (i) it can handle the nonlinear wind

turbine dynamics, (ii) the wind turbine rotor dynamics under the planned power generation strategy is guaranteed to be asymptotically stable, (iii) the computational cost is low, and (iv) the algorithm is scalable in terms of the CPU time, i.e. the computational cost is maintained to be approximately the same as the number of wind turbines in a farm increases. The algorithm has practical usefulness in power planning of wind farms and shows a novel approach. There is still scope in this work for future work directions and the next section will discuss several future work options.

Future Work

There are a few directions that can be taken in the future extensions of the current work:

1) Use of different models: Since the method can handle non homogeneous models, other models can be substituted in the work. The Jensen wake model can be substituted with other models to perform the wake loss calculation. The Jensen model is a rather simple model and assumes a linearly expanding wake, the velocity deficit in the model is solely dependent on distance and does not consider turbulence (Renkema, 2007). A 2D or 3D field model (Renkema, 2007) can be considered and can provide more accurate wind information. The wind turbines in the wind farm can be of other properties and sizes. The generator torque control strategy can also be modified as the part of future work. In the current simulations an optimal generator torque strategy was used.
2) The layout of wind farms are dictated more by grid connections and installation costs than wake losses, some power loss due to wake is accepted in place of higher costs. The simulations in the present work used an array type wind farm, but the algorithm can also be used for other types of wind farm layouts. In land based wind farms it is harder to have a

uniform layout because of terrain and other structures in the landscape, the algorithm can also be applied to such wind farms for future work. A wind farm with less uniform wind turbine placement would also involve a more complicated wake calculation and may increase the planning time of the algorithm. The CPU time for the upper level is expected to increase in such an irregular wind farm, but the CPU time for the lower level should remain unchanged.

3) Another direction could be in studying the effect of initial SPC setting. In the simulations shown and proofs it was found that a higher SCP setting gave a faster convergence to the desired power.
4) The algorithm can be ran on a more powerful computer system and a more powerful programming language and that is expected to reduce the computational cost even more.
5) Study and add effects of noise in wind velocity, pitch actuator in the coordinated power planning of wind turbines in a wind farm.
6) Experimental verification of the modified local pursuit inspired power planning of wind farms can be conducted on test bed of wind turbines. For such verification a scaled down model of wind turbine can be used. For a scaled down wind turbine for use in wind tunnels servo motors can be used for pitch control. For smaller size wind turbines, variable speed generators are not possible and for such scaled down wind turbines, DC generators will be used. This will make the wind turbine a variable pitch fixed speed wind turbine. In a test wind tunnel wind turbine rows can be placed, for the verification of algorithm, a small wind farm array can be setup with a 2x2 configuration and perhaps 4x4 if the wind tunnel is big enough.

7) In the current work the open loop planning stability analysis assumed that the model is perfectly known and there are no sensor/actuator noise or uncertainties. In future work the effect of uncertainties on the planning algorithm can be studied, and a robustness analysis can be done of the method. Stability analysis can also be done with noise considered.

LIST OF REFERENCES

Choosing a solver, http://www.mathworks.com/help/optim/ug/choosing-a-solver.html#brhkghv-19, last accessed in May 2015.

Fahroo, F., and Ross, I. M., (2001), 'Costate Estimation by a Legendre Pseudospectral Method,' *Journal of Guidance, Control, and Dynamics*, 24, pp. 270-275.

Fernandez, R. D., Battaiotto, P. E., and Mantz, R. J., (2008), 'Wind Farm Nonlinear Control for Damping Electromechanical Oscillations of Power Systems,' *Renewable Energy*, 33(10), pp. 2258–2265.

Gipe, P., (2004), Wind Power: Renewable Energy for Home, Farm, and Business, Chelsea Green Publishing Company, White River Junction, VT.

Hau, E., (2012), Wind Turbines: Fundamentals, Technologies, Application, Economics, Springer, Heidelberg, Germany.

Hristu-Varsakelis, D. and Shao, C., (2004), 'Biologically-inspired Optimal Control: Learning from Social Insects,' *International Journal of Control*, 77(18), pp. 1549-1566.

Hui, J. and Bakhshai, A., (2008), 'A New Adaptive Control Algorithm for Maximum Power Point Tracking for Wind Energy Conversion Systems,' *The Proceedings of IEEE Power Electronics Specialists Conference*, Rhodes, Greece, June 15-19, pp. 4003-4007.

Jelavić, M., Perić, N., & Petrović, I., (2007), 'Damping of wind turbine tower oscillations through rotor speed control,' *CD-ROM Proceedings of the Ecologic Vehicles and Renewable Energies International Exhibition and Conference-EVER*, Monaco, March 29-April 1.

Johnson, K. E., and Thomas, N., (2009), 'Wind Farm Control: Addressing the Aerodynamic Interaction among Wind Turbines,' *American Control Conference*, St. Louis, MO, June 10-12, pp. 2104-2109.

Jonkman, J., Butterfield, S., Musial, W., and Scott, G., (2009), 'Definition of a 5-MW Reference Wind Turbine for Offshore System Development,' *National Renewable Energy Laboratory: NREL/TP-500-38060*, February 2009.

Knudsen, T., Bak, T. and Svenstrup, M., (2014), 'Survey of Wind Farm Control - Power and Fatigue Optimization,' *Wind Energy*, URL http://dx.doi.org/10.1002/we.1760

Madjidian, D., Kristalny, M., and Rantzer, A., (2013), 'Dynamic Power Coordination for Load Reduction in Dispatchable Wind Power Plants,' *European Control Conference*, Zurich, Switzerland, July 17-19, pp. 3554-3559.

Marden, J. R., Ruben, S. D., and Pao, L. Y., (2013), 'A Model-free Approach to Wind Farm Control using Game Theoretic Methods,' *Control Systems Technology*, *IEEE Transactions*, 21(4), July, pp. 1207-1214.

Munteanu, I., Cutululis, N. A., Bratchu, A. I. and Ceanga, E., (2005), 'Optimization of Variable Speed Wind Power Systems based on a LQG Approach,' *Control Engineering Practice*, 13(7), July, pp. 903-912.

Offshore Wind Energy, http://www.boem.gov/renewable-energy-program/renewable-energy-guide/offshore-wind-energy.aspx, last accessed in November 2013.

Pao, L. Y., and Johnson, K. E., (2011), 'Control of Wind Turbines: Approaches, Challenges, and Recent Developments,' *IEEE Control Systems Magazine*, 31(2), April, pp. 44-62.

Park, J., Kwon, S., and Law, K. H., (2013), 'Wind Farm Power Maximization based on a Cooperative Static Game Approach,' *Proceedings of the SPIE Smart Structures/NDE Conference,* Vol. 8686, San Diego, CA, March 12-13, pp. 1-15.

Renkema, D. J., (2007), 'Validation of Wind Turbine Wake Models: Using Wind Farm Data and Wind Tunnel Measurements,' Master of Science Thesis, Delft University of Technology, June 11.

Sandia Labs News Releases, SWiFT Commissioned to Study Wind Farm Optimization, https://share.sandia.gov/news/resources/news_releases/swift-wind-farm-optimization/#.UzebrfldWSp, last accesed in November 2013.

Schreck, S., Lundquist, J. and Shaw, W., (2008), 'Research Needs for Wind Resource Characterization,' *Bulletin of the American Meteorological Society*, 90(4), pp. 535-538.

Senjyu, T., Ryosei, S., Naomitsu, U., Funabashi, T., and Sekine, H, (2006), 'Output Power Leveling of Wind Farm using Pitch Angle Control with Fuzzy Neural Network,' *Power Engineering Society General Meeting*, Montreal, Canada.

Semrau, G., Rimkus, S., and Das, T., (2015) 'Nonlinear Systems Analysis and Control of Variable Speed Wind Turbines for Multiregime Operation,' *ASME Journal of Dynamic Systems, Measurement, and Control*, 137(4), April 1, pp. 041007-1 – 041007-10.

Slotine, J. J. and Li, W., (1991), Applied Nonlinear Control, Prentice Hall, Englewood Cliffs, NJ.

Soleimanzadeh, M., Brand, A. J. and Wisniewski, R., (2011), 'A Wind Farm Controller for Load and Power Optimization in a Farm,' *The 2011 IEEE International Symposium on Computer-Aided Control System Design,* Denver, CO, September 28-30, pp. 1202-1207.

Skolthanarat, S., (2009), 'The Modeling and Control of a Wind Farm and Grid Interconnection in a Multi-machine system,' PhD dissertation, Virginia Polytechnic Institute and State University.

Sorensen, P., Ejnar, A., Hansen, D., Janosi, L., Bech, J., and Bak-Jensen, B, (2002), 'Simulation of Interaction between Wind Farm and Power System,' Riso National Laboratory, Roskilde, Denmark.

Spudic, V., Baotic, M. and Peric, N., (2011), 'Wind Farm Load Reduction via Parametric Programming based Controller Design,' *Proceedings of the 18th IFAC World Congress*, 18(1), Milano, Italy, pp.1704-1709.

Spudic, V., Jelavic, M., Baotic, M. and Peric, N., (2010), 'Hierarchical Wind Farm Control for Power/Load Optimization,' *Proceedings of the Science of Making Torque from Wind*, Heraklion, Greece.

Spudic, V., Jelavic, M., Baotic, M. and Vasak, M., (2010),'Distributed Control of Large - Scale Offshore Wind Farms (AEOLUS), Technical Report, University of Zagreb.

van Dam, F., Gebraad, P., and van Wingerden, J. W., (2012), 'A Maximum Power Point Tracking Approach for Wind Farm Control,' *Proceedings of The Science of Making Torque from Wind*, Oldenburg (Oldb), Germany.

Van der Hooft, E. L., Schaak, P., and Van Engelen, T. G., (2003), 'Wind turbine control algorithms,' *DOWEC project-DOWEC-F1W1-EH-03-094/0, Task-3 report.*

Wang, Z., Cai, C., and Jia, K., (2013), 'Neural Network Adaptive Control for Constant Output Power of Variable Pitch Wind Turbine,' *The 2013 IEEE International Conference on Vehicular Electronics and Safety*, Dongguan, China, July 28-30, pp.165-170.

Wind turbine 3D model, http://www.3dcadbrowser.com/download.aspx?3dmodel=20363, last accessed in May 2015.

Xu, Y., Remeikas, C., and Pham, K., (2013), 'Local Pursuit Strategy Inspired Cooperative Trajectory Planning Algorithm for a class of Nonlinear Constrained Dynamical Systems,' *International Journal of Control*, 87(3), pp. 506-523.